Contains Proprietary information
from SIA and Framatome

Failure Criterion Development and Parametric Finite Element Analyses to Assess Margins for the Davis-Besse RPV Head Corrosion

by

G. Wilkowski, R. Wolterman, D. Rudland, and Y.-Y. Wang
Engineering Mechanics Corporation of Columbus

April 30, 2002
to
U.S. NRC – RES

EXECUTIVE SUMMARY

This report estimates the margins that existed for the cladding in the Davis-Besse head wastage case. The margins on the calculated "failure pressure" to the operating pressure were calculated, as well as the amount of additional corrosion that had to occur for failure at the normal operating pressure.

The development of the failure criterion is first presented. The "best-estimate failure criterion" was defined as the pressure that produced the equivalent strain under biaxial loading equal to an average critical value through the thickness in the cladding. The basis of the "best-estimate failure criterion" is that the equivalent critical strain under biaxial loading corresponds to the ultimate stress in a uniaxial tension test. This resulted in the "critical equivalent strain" being 5.5 percent under biaxial loading rather than the 11.2 percent strain in the uniaxial tensile test at the start of necking. An additional consideration is needed to account for the strain gradient through the cladding thickness. When the critical strain is exceeded, then there is a redistribution of stresses that is not accounted for in the finite element analysis. To account for this lack of stress redistribution, it was assumed that failure would be reached when the average strain in the thickness exceeded the critical strain. The best-estimate "failure pressures" gave margins of 1.07 to 1.39 on the normal operating pressure. This agreed well with estimated results from the SIA analysis when the same failure criterion was used. Preliminary results from ORNL gave a higher calculated failure pressures with the same criterion, but further mesh refinement in the clad region is being pursued. The estimated additional corrosion needed to cause failure at the normal operating pressure was 0.9 to 1.8 inches more in the longest dimension when using our "best-estimate failure criterion".

The "best-estimate failure criterion" developed in this report gives calculated "failure pressures" that are about a factor of 2.2 lower than the failure criterion used in the SIA report.

These results could be affected by: (1) variable thickness (the average thickness was used in the values given above), (2) potential cladding flaws, (3) the failure strain being lower due to void growth under higher triaxial stresses causing a reduction in the ultimate strength, (4) the assumption of failure occurring when the average strain though the thickness exceeds the critical strain, (5) variability in the stress-strain curve (the curve used appeared to be an average not a minimum), and (6) a different thickness gradient along the transition from the clad region to the full head thickness than what was used.

It is recommended that the cladding to head thickness transition be documented in the metallographic work to be done once the area is cut out from the head. If a more precise assessment is desired, then the failure criterion should be explored further.

4-H-98

INTRODUCTION

In March of 2002, the Davis-Besse nuclear power plant shut down early for an inspection of potential cracks in control-rod nozzles in the reactor pressure vessel head. This inspection was required by the U.S.NRC due to concerns of circumferential cracks that had occurred at other nuclear plants that were also manufactured by B&W. During that inspection, several axial cracks were found using an under-the-head UT inspection technique. The insulation on top of the head made the visual inspection of boric acid deposits difficult.

While making a repair of a cracked nozzle by partially machining the tube away so that a new weld could be made at the mid-thickness region of the head, it was found that a significant part of the head around that nozzle had corroded away. In some regions, the corrosion was completely down to the cladding, so that only the nominal design 3/16" thick cladding was maintaining the pressure in the vessel. (The actual thickness was greater than the nominal thickness.)

The occurrence of this magnitude of corrosion raised considerable concern at the NRC. One aspect that was desired to know was how close the head was to failure. Failure in this case would have resulted in a rupture of the cladding causing an opening area equal to or less than the clad-only region. This would have constituted a small to medium-break LOCA that could have been mitigated by the emergency core cooling system and containment building to prevent release of the pressurized water to the outside environment. Hence, the objective of this report was to develop a quick assessment of the margin that might have existed. To make this quick assessment, a 2-dimensional parametric finite element analysis procedure was developed to allow the NRC to make an assessment of the margins that might have existed for the Davis-Besse corroded head.

Figure 1 shows a photograph of the corroded area from above the head. This picture shows where the 4-inch outside diameter CRDM tube was, and to the left an area where the entire thickness of the head had corroded down to the stainless steel cladding. The nominal design 3/16" thick cladding had held the internal pressure during some significant time period. After significant investigation and daily conference calls on this matter between the NRC, Davis-Besse staff, and their consultants, it was determined that the precise geometry of how the cladding-only area transitioned to the head was difficult to obtain. Due to the safety significance of this situation, Engineering Mechanics Corporation of Columbus (Emc^2) was asked to assist the NRC in determining the margins that existed for this case.

Analyses undertaken for the U.S. NRC by Emc^2 are presented in this report, as well as comparisons to SIA results and preliminary results from ORNL.

Some of the information used in this report was proprietary information from Framatome and SIA.

We would also like to than the following for their assistance and input; Prof. Mark Tuttle, University of Washington, Prof. Tony Atkins, Reading University – UK, Professor Jwo Pan, University of Michigan, and Dr. Raj Mohan, Rouge Steel.

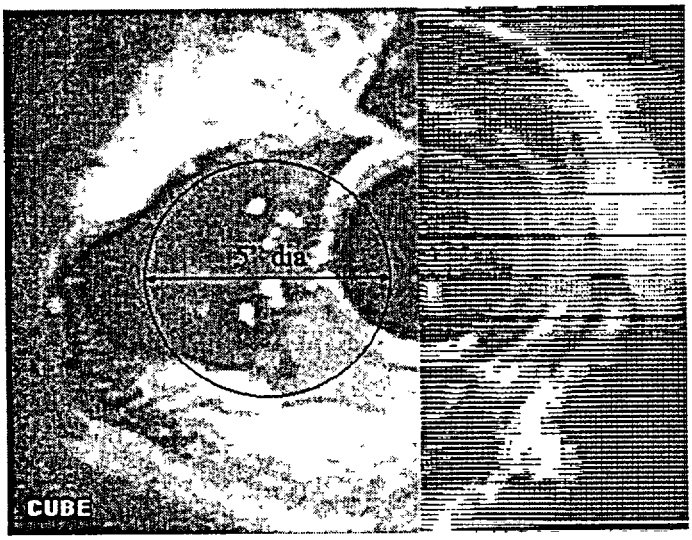

Figure 1 Photograph showing corroded area in Davis-Besse head

APPROACH

The approach undertaken in this report was to assess the cladding "failure" pressure in the corroded area using 2-dimensional finite element analysis procedures. Existing gas pipeline pipe corrosion failure models exist, but they are typically not very accurate for deep corrosion flaws.[1,2] A similar limitation exists for flaw assessment criteria in ASME Section XI, i.e., Code Case N-597. The ratio of depth of the corrosion compared to the thickness of the head was about 0.95, which is beyond the validity range of existing corrosion models.

Consequently, the approach in this effort was to conduct a number of axisymmetric finite element analyses that will allow the NRC to bound the failure pressure for the actual case. The analyses undertaken in this report involved large-deformation finite element analyses of a full reactor pressure vessel head with a single axisymmetric corrosion pit down to the cladding. The diameter of the corroded area and the thickness of the cladding were variables in these analyses.

In this case, the Davis-Besse low-alloy steel head had a thickness of 6 and 13/16 inches (including the cladding) according to FirstEnergy's submittal to NRC Bulletin 2001-01 (Docket Number 50-346). The cladding had a nominal design thickness of 3/16 inch according to the same submittal. The cladding maximum design thickness was 3/8 inch, and the design minimum thickness was 1/8 inch thick. Davis-Besse staff reported to the NRC staff that the measured cladding thickness in the corroded area had an average thickness of 0.297 inch with a minimum value of 0.24 inch.

---

[1] Kiefner, J. F., and Duffy, A. R., "Criteria for Determination the Strength of Corroded Areas of Gas Transmission Lines," presented at 1973 American Gas Association Transmission Conference. (Technical basis for ASME B31G.)
[2] D. Stephens and B. Leis, "Development of an Alternative Criterion for Residual Strength of Corrosion Defects in Moderate- to High-Toughness Pipe", Proceedings of 2000 International Pipeline Conference, Vol. 2, pp. 781-792, October 2000.

The finite element analyses only determine the pressure-strain relationship. Since the analyses do not include elements that simulate necking (i.e., Gurson elements in ABAQUS require additional material parameters, e.g., initial inclusion size and spacing distributions, that are unknown at this time for the cladding material), a failure criterion needs to be established to estimate a failure pressure from the stress analysis. Although it is generally agreed that the failure will be a plastic collapse (or limit-load) of the cladding, the details in selection of the failure criterion are important. Hence, the following section discusses the "Failure Criterion" aspects. The next section gives the description of the finite element analyses. The final section gives the critical pressure diagrams for cases of varying the diameter of the corroded area, the thickness, and different "failure criteria", with an assessment of the margins that might have existed for the Davis-Besse cladding. Detailed pressure versus strain plots are given in Appendices A and B.

FAILURE CRITERION

A reasonable suggestion is that the "failure criterion" for the cladding in the corroded area involves a limit-load analysis. In the industrial analysis submitted to date[3], it was assumed that failure would occur in the cladding once it reached the true strain that corresponds to the ultimate strength from uniaxial tensile test data of cladding weld metal at 600F.

Two assessments were made of this "failure criterion" assumption. (1) We compared their TP308 stress-strain curve to data from past NRC piping programs where all-weld-metal 308 stress-strain curves were developed, and (2) the assumption that the uniaxial strain at ultimate stress could be used was assessed. The reason for the second assessment was that biaxial loading might change the equivalent strain at the start of necking, where necking occurs when the limit-load pressure is reached.

Comparison of Framatome Cladding Stress-Strain Curve to Past Data

A stress-strain curve for TP308 cladding weld metal was sent from Framatome so that NRC contractors and industry contractors would be using similar material properties in their analyses. The cladding is a submerged arc weld (flux based rather than inert gas welding). The data was for a uniaxial tensile test, and came from "raw engineering tensile data at 600 F (minimum) from *Nuclear Systems Materials Handbook*, Vol. 1 Design Data, Section 1A, for TP308/TP308L weld." Although not stated, it probably came from a round-bar tensile test.

A significant number of TP308 weld metal tensile tests were also conducted during the various NRC pipe fracture programs. The data in the latest version of the PIFRAC[4] database was for tests only up to 550F, so that these stress-strain curves might be slightly higher than the 600F data. Figure 2 and Figure 3 show comparisons of the Framatome supplied TP308-weld-metal stress-strain curve (at 600F) to the data from the PIFRAC database (at 550F). As can be seen in Figures 2 and 3, the Framatome supplied 600F data is higher than several of the curves from the PIFRAC database, and there are a few specimens with lower strains at ultimate. If the PIFRAC materials were tested at 600F, it is expected that the stress values might be slightly lower than shown in Figures 2 and 3. Hence, the Framatome stress-strain curve data falls closer to the mean value of the PIFRAC data, but is not necessarily a minimum bounding curve.

---

[3] SIA Report on "Operability and Root Cause Evaluation of the Damage of the Reactor Pressure Vessel Head at Davis-Besse – Elastic-Plastic Finite Element Stress Analysis of Davis-Besse RPV Head Wastage Cavity," File No. W-DB-01Q-301, Project No. W-DB-01Q, April 2, 2002.

[4] Ghadiali, N., and Wilkowski, G. M., "Fracture Mechanics Database for Nuclear Piping Materials (PIFRAC)," in *Fatigue and Fracture - 1996 - Volume 2*, PVP - Vol. 324, July 1996, pp. 77-84.

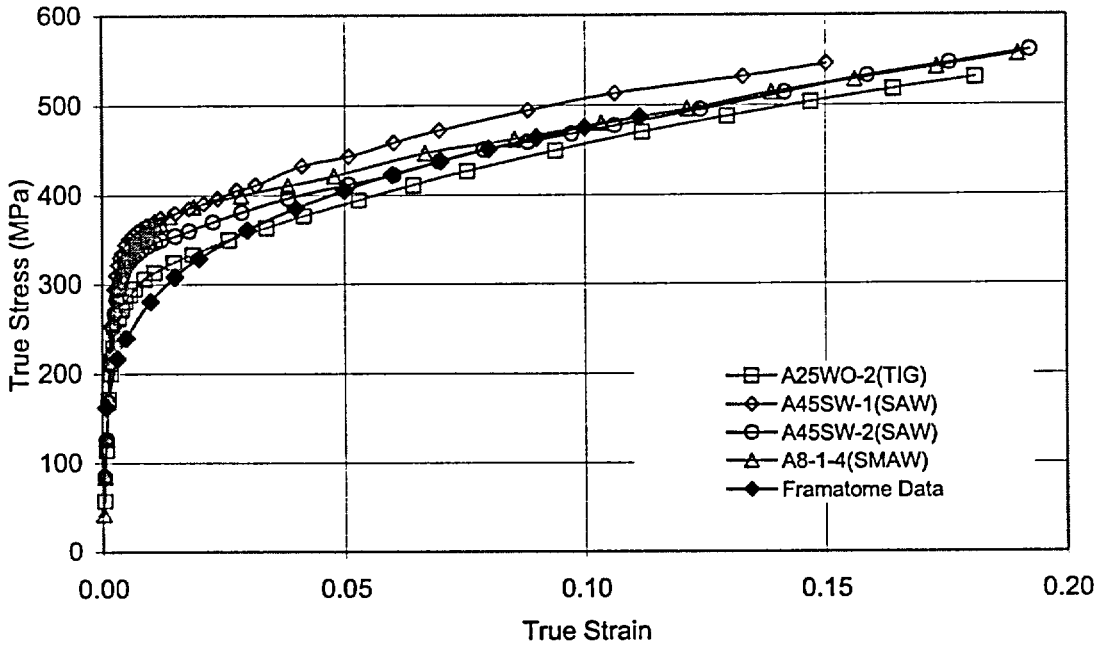

Figure 2 Comparison of TP308 weld metal uniaxial stress-strain curves (Framatome at 600F, others at 550F)

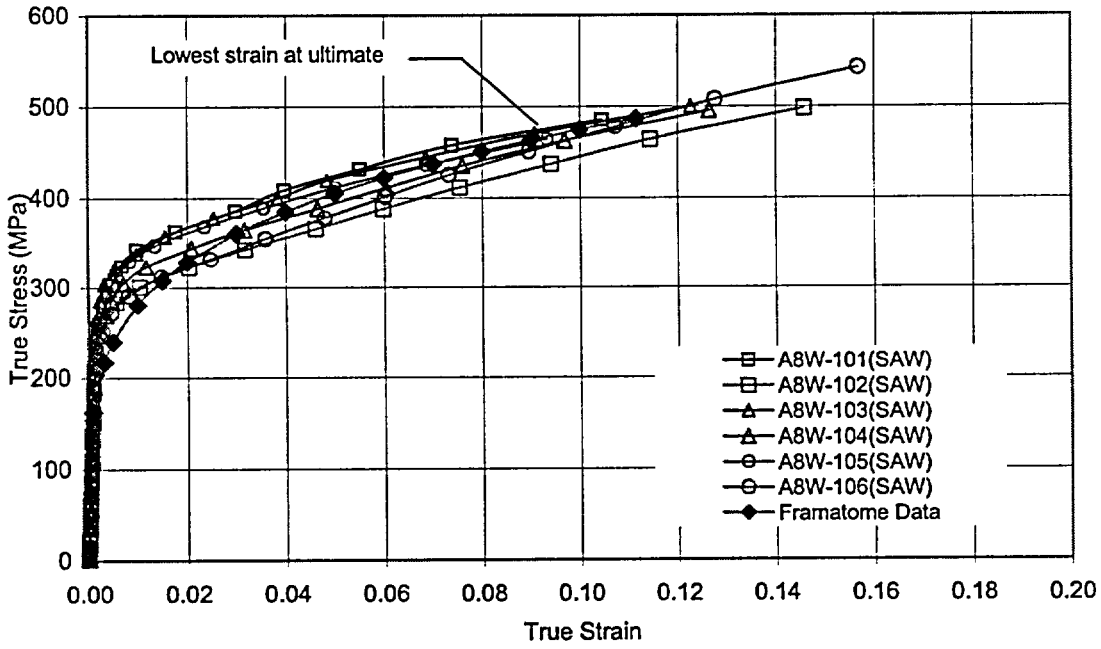

Figure 3 Comparison of TP308 weld metal uniaxial stress-strain curves (Framatome at 600F, others at 550F)

Assessment of Strain Limit for "Failure" Criterion

In material behavior, plastic instability can be defined as a severe localization of the plastic deformation in the material due to a decrease in cross-sectional area. Many researchers have modeled this behavior, which is a function of the equivalent stresses and strains in the material. Limit-forming diagrams are frequently used in the automotive and shipbuilding industries to make sure sheets of steel do not locally neck (wrinkle) under the biaxial stresses of forming. Invariably, everyone that was contacted agreed that the equivalent failure strain under biaxial loading would be lower than under uniaxial loading. No precise data found in this short time-period (a literature survey was started, but was not available at the time of this report) for TP308 stainless steel weld metal under biaxial loading.)

The failure that occurs after localized necking can be described in damage mechanics terms. The void formation that occurs in the necked region is a function of the initial inclusion distribution, as well as the triaxial stress state and the magnitude of plastic strains. For example, biaxial loading may increase the triaxial stress state but decrease the plastic flow when compared to uniaxial loading. Therefore, an understanding of each phenomenon is important when determining the failure under biaxial loads.

To determine the decrease in the plastic flow due to biaxial loads, a relationship between the stresses and the strains during the biaxial loading needs to be developed. This development is given in the next section Using this relationship, the plastic strain limit under biaxial loading can be determined.

The decrease in the equivalent stress at the onset of necking, due to the increase in triaxiality of the stress state when going from uniaxial to biaxial loading, is more difficult to quantify. Logically, the triaxial stress state is the larger contributor to the void growth behavior, and may overcome the compensating effects of having the lower plastic strains. There was not sufficient time to explore this aspect, and some test data on the cladding material under biaxial material may be needed to properly assess the "failure criterion", whether it is used in this analysis or more detailed analyses by ORNL.

For this initial investigation, it was decided that failure would be defined as the equivalent plastic strain under biaxial loading that corresponds to the stress at the onset of necking in a uniaxial test specimen.

Finally, it should be noted that inclusions in flux welds are well known to reduce the ductile fracture toughness due to crack tip void growth. Similarly, necking (void growth) may start earlier in the flux weld metal under equal (1:1) biaxial loading because of the inclusion content is higher for a flux weld than an inert gas weld.

Development of a Constitutive Relationship Under 1:1 Biaxial Loads

The analysis that follows is described in Dowling, N.E., *Mechanical Behavior of Materials*, 1st Ed, Prentice Hall, 1993, ISBN 0-13-579046-8, Section 12.3.4.[5]

For substantial yielding up to ultimate stress levels, assume the total strains can be viewed as the sum of elastic and plastic components:

$$\varepsilon_{total} = \varepsilon_e + \varepsilon_p \tag{1}$$

The biaxial stress is a plane-stress state, so assume the stress is referenced to the principal stress coordinate system:

[5] Input provided by Prof. M. Tuttle of University of Washington.

$$\sigma_1 = \sigma_x \qquad \sigma_2 = \sigma_y \qquad \sigma_3 = \sigma_z = 0 \qquad \tau_{xy} = \tau_{xz} = \tau_{yz} = 0$$

For convenience, define:

$$\sigma_2 = \lambda \sigma_1$$

The elastic strain is given by the Hooke's law for plane stress:

$$\begin{aligned} \varepsilon_{1e} &= \frac{1}{E}[\sigma_1 - \nu(\sigma_2 + \sigma_3)] = \frac{\sigma_1}{E}(1 - \nu\lambda) \\ \varepsilon_{2e} &= \frac{1}{E}[\sigma_2 - \nu(\sigma_1 + \sigma_3)] = \frac{\sigma_1}{E}(\lambda - \nu) \\ \varepsilon_{3e} &= \frac{1}{E}[\sigma_3 - \nu(\sigma_1 + \sigma_2)] = \frac{-\nu\sigma_1}{E}(1 + \lambda) \end{aligned} \tag{2}$$

Where E and ν are the elastic values of Young's modulus and Poisson's ratio, respectively.

The plastic strains are given as:

$$\begin{aligned} \varepsilon_{1p} &= \frac{1}{E_p}\left[\sigma_1 - \frac{(\sigma_2 + \sigma_3)}{2}\right] = \frac{\sigma_1}{E_p}\left(\frac{2 - \lambda}{2}\right) \\ \varepsilon_{2p} &= \frac{1}{E_p}\left[\sigma_2 - \frac{(\sigma_1 + \sigma_3)}{2}\right] = \frac{\sigma_1}{E_p}\left(\frac{2\lambda - 1}{2}\right) \\ \varepsilon_{3p} &= \frac{1}{E_p}\left[\sigma_3 - \frac{(\sigma_1 + \sigma_2)}{2}\right] = \frac{-\sigma_1}{2E_p}(1 + \lambda) \end{aligned} \tag{3}$$

Where E_p is the "plastic modulus", defined by:

$$E_p = \frac{\bar{\sigma}}{\bar{\varepsilon}_p} \tag{4}$$

$\bar{\sigma}$ = the "effective stress" (closely related to the octahedral shear stress)

$\bar{\varepsilon}_p$ = the "effective plastic strains" (closely related to the octahedral shear plastic strain)

Also, the above expression assumes that the Poisson ratio relating stress to plastic strains is 1/2, which is true for most metals.

In general:

$$\bar{\sigma} = \frac{1}{\sqrt{2}}\sqrt{(\sigma_1 - \sigma_2)^2 + (\sigma_2 - \sigma_3)^2 + (\sigma_3 - \sigma_1)^2}$$

For the particular case of plane stress ($\sigma_2 = \lambda\sigma_1, \sigma_3 = 0$):

$$\bar{\sigma} = \sigma_1\sqrt{1 - \lambda + \lambda^2} \tag{5}$$

The effective total strain is related to the effective stress and effective plastic strain according to:

$$\bar{\varepsilon} = \frac{\bar{\sigma}}{E} + \bar{\varepsilon}_p$$

This is valid for *any* state of stress (including biaxial stress states). Various models have been proposed that relate the effective stresses and strains for the *particular* case of a uniaxial state of stress. For the moment, denote the model used to describe the uniaxial stress-strain curve as:

$$\bar{\varepsilon} = f(\bar{\sigma})$$

(Calculations will be presented below based on the Ramberg-Osgood model, i.e., the function $f(\bar{\sigma})$ that will be used below is the one proposed by Ramberg-Osgood).

Solving for the effective plastic strains:

$$\bar{\varepsilon}_p = f(\bar{\sigma}) - \frac{\bar{\sigma}}{E} \tag{6}$$

Combining Equations (1) - (6) gives (after some algebra):

$$\begin{aligned}
\varepsilon_1 &= \frac{\lambda\sigma_1}{E}\left(\frac{1-2\nu}{2}\right) + \frac{(2-\lambda)}{2\sqrt{1-\lambda+\lambda^2}} f(\bar{\sigma}) \\
\varepsilon_2 &= \frac{\sigma_1}{E}\left(\frac{1-2\nu}{2}\right) + \frac{(2\lambda-1)}{2\sqrt{1-\lambda+\lambda^2}} f(\bar{\sigma}) \\
\varepsilon_3 &= \frac{\sigma_1}{E}\frac{(1-2\nu)(1+\lambda)}{2} - \frac{(1+\lambda)}{2\sqrt{1-\lambda+\lambda^2}} f(\bar{\sigma})
\end{aligned} \tag{7}$$

The functional form of $f(\bar{\sigma})$ must now be specified. The Ramberg-Osgood function is:

$$f(\bar{\sigma}) = \frac{\bar{\sigma}}{E} + \left(\frac{\bar{\sigma}}{H}\right)^{1/n}$$

Where, n = "strain hardening exponent" (a material constant)
H = a material constant

Using this form in Eq. (7) and simplifying:

$$\begin{aligned}
\varepsilon_1 &= \frac{\sigma_1}{E}(1-\nu\lambda) + \left(\frac{2-\lambda}{2}\right)\left(1-\lambda+\lambda^2\right)^{[(1-n)/2n]}\left(\frac{\sigma_1}{H}\right)^{1/n} \\
\varepsilon_2 &= \frac{\sigma_1}{E}(\lambda-\nu) + \left(\frac{2\lambda-1}{2}\right)\left(1-\lambda+\lambda^2\right)^{[(1-n)/2n]}\left(\frac{\sigma_1}{H}\right)^{1/n} \\
\varepsilon_3 &= \frac{-\nu\sigma_1}{E}(1+\lambda) - \left(\frac{1+\lambda}{2}\right)\left(1-\lambda+\lambda^2\right)^{[(1-n)/2n]}\left(\frac{\sigma_1}{H}\right)^{1/n}
\end{aligned} \tag{8}$$

If the stress state is uniaxial ($\lambda = 0$), then Eq. (8) reduces to:

$$\varepsilon_1 = \frac{\sigma_1}{E} + \left(\frac{\sigma_1}{H}\right)^{1/n}$$

$$\varepsilon_2 = \varepsilon_3 = \frac{-\nu\sigma_1}{E} - \left(\frac{1}{2}\right)\left(\frac{\sigma_1}{H}\right)^{1/n} \tag{9}$$

The equivalent strain can be calculated using the distortion energy theory definition:

$$\bar{\varepsilon} = \frac{2}{3}\sqrt{(\varepsilon_1 - \varepsilon_2)^2 + (\varepsilon_2 - \varepsilon_3)^2 + (\varepsilon_3 - \varepsilon_1)^2} \tag{10}$$

Using the above equations, the material response under uniaxial and biaxial loading can be compared. If it assumed that failure occurs at the same stress level, the decrease in failure strain due to the biaxial loading can be determined. The properties supplied by Framatome for the stainless steel TP308 weld metal are as follows:

Test temperature, F	600
0.2% yield strength, ksi	30.9
Ultimate strength, ksi	62.3
Uniform elongation	11.8%
Total elongation (not plotted)	20.6%

Using a Ramberg-Osgood curve fit the constants are as follows:

H = 115 ksi
n = 0.228

with

E = 25,570 ksi
ν = 0.295

The uniaxial stress-strain relationship is given below:

Table 1 Uniaxial stress-strain curve values from Framatome for TP308 weld metal at 600F

True strain	True stress, ksi
0	0.00
0.20%	30.96
0.50%	37.24
1.00%	42.83
1.50%	46.48
2.00%	49.25
3.00%	53.45
4.00%	56.64
5.00%	59.25
6.00%	61.47
7.00%	63.41
8.00%	65.14
9.00%	66.70
10.00%	68.13
11.15%	69.65

Using these constants and Equations 8 and 10, an estimate of the uniform equivalent strain up to the same ultimate stress under biaxial loading can be made. Letting λ=1 and plotting the equivalent strains, the difference between uniaxial and biaxial loading can be seen in Figure 4. The results indicate that if the ultimate stress is used, the equivalent strain decreases significantly when the mode of loading is biaxial tension, i.e., the uniaxial value of 11.15% strain decreases to 5.5% for biaxial loading.

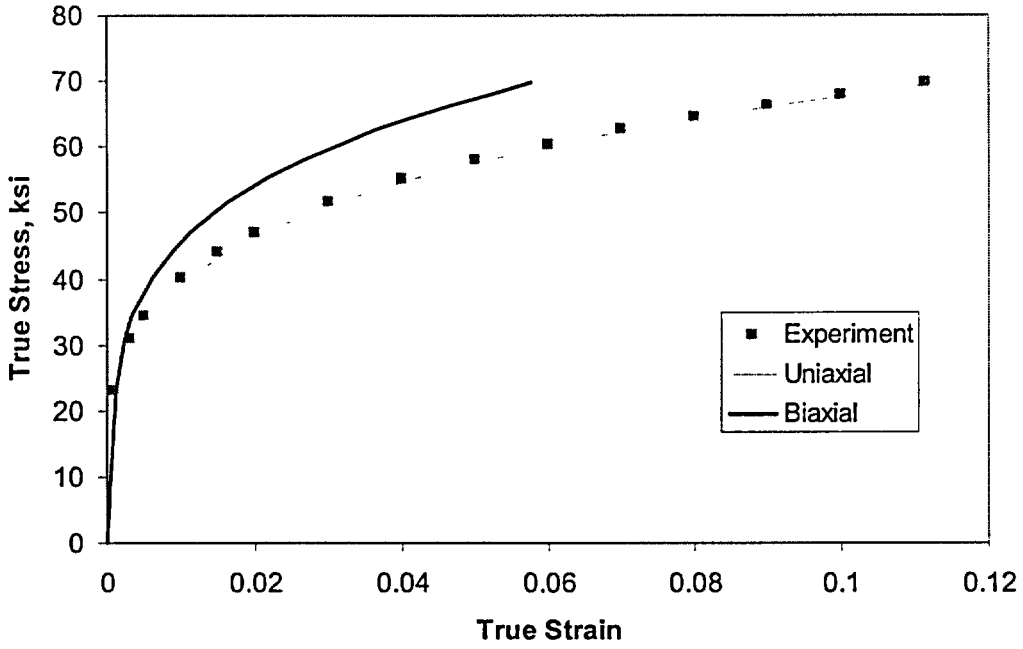

Figure 4 Comparison of uniaxial and calculated biaxial stress-strain curves for TP308 weld metal at 600F

Critical Strain Evaluation from Spherical Shell Analysis

The section describes the conditions for maximum load in uniaxial tension and conditions for maximum internal pressure for a thin-walled sphere under internal pressure, as was developed by McClintock[6]. From the maximum load conditions in this analysis, the critical strain can be determined. Since a thin-walled sphere under pressure loading is close to pure 1:1 biaxial loading, with equal stress components, this analysis provides additional support to the critical biaxial strain criterion to be used.

The conditions for maximum load in uniaxial tension is given in terms of equivalent plastic strain versus equivalent stress relation,

$$\sigma_e = \frac{d\sigma_e}{d\varepsilon_e^p} \tag{11}$$

where σ_e is the equivalent stress and ε_e^p is the equivalent plastic strain.

Assume the equivalent stress-strain relation follows the following form,

$$\sigma_e = \sigma_{e1}\left(\varepsilon_e^p\right)^n \tag{12}$$

[6] McClintock, F.A. and Argon, A.S., "Mechanical Behavior of Materials," Addison-Wesley Publishing Company, ISBN 0-201-04545-1.

where σ_{e1} and n are fitted parameters.

Applying Eq. (12) to Eq. (11), it may be obtained that the maximum load occurs at $\varepsilon_e^p = n$. Therefore, the equivalent stress at the maximum load is $\sigma_e^{uni} = \sigma_{e1} * n^n$.

In a thin-walled sphere, the condition for maximum load is,

$$1.5\sigma_e = \frac{d\sigma_e}{d\varepsilon_e^p} \tag{13}$$

Applying Eq. (12) to Eq. (13), it may be obtained that the maximum pressure occurs at $\varepsilon_e^p = n/1.5$. Therefore, the equivalent stress at the maximum pressure is $\sigma_e^{pre} = \sigma_{e1} * \left(\frac{n}{1.5}\right)^n$. We have,

$$\frac{\sigma_e^{uni}}{\sigma_e^{pre}} = 1.5^n \tag{14}$$

Using Eq. (14) and a value of n = 0.228 as previously discussed, it is estimated that

$$\frac{\sigma_e^{uni}}{\sigma_e^{pre}} = 1.097$$

In other words, the equivalent stress at maximum pressure is 91% of the equivalent stress at the maximum load of a uniaxially loaded specimen. This gives an equivalent strain of 7.0 percent.

Strain Gradient Effects

An additional consideration that can be significant is the effect of a strain gradient in the ligament. There are three different possibilities. Failure occurs when:

1. The entire ligament exceeded the "critical strain" value selected (SIA used this approach with 11.2% strain, i.e., the 11.2% minimum strain criterion), or
2. When the average strain in the ligament reached the "critical strain" (Emc^2 used this approach with the 5.5% average strain criterion), or
3. When any point in the ligament first reached the "critical strain" (i.e., the maximum strain criterion).

These three failure criteria are illustrated in Figure 5, which shows the calculated strain gradients through the thickness of a typical finite element analysis.

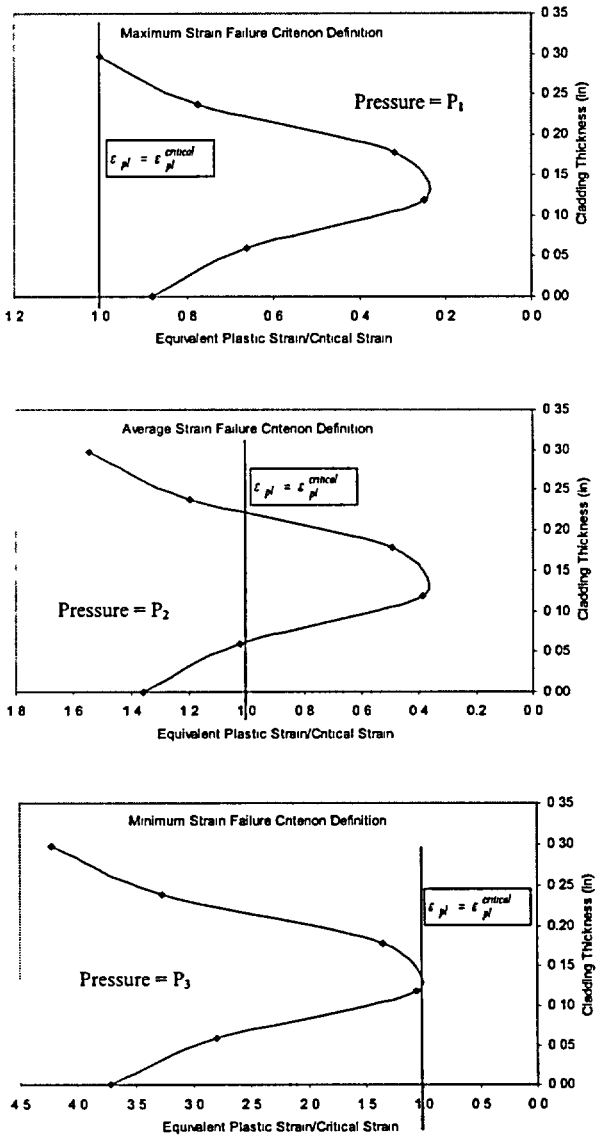

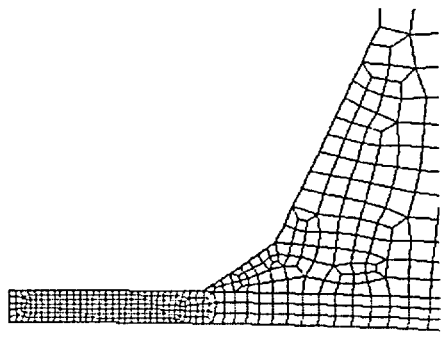

Close-up of remaining ligament of cladding showing five elements through the thickness

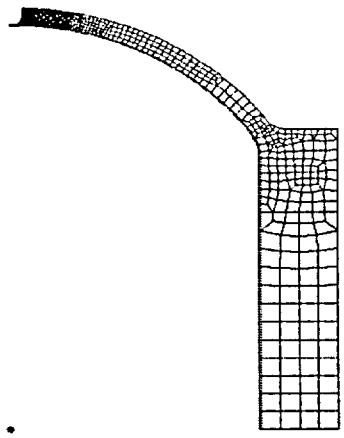

Axisymmetric finite element model showing remaining ligament at upper left corner.

Figure 5 Plots typical of the strain profile through the thickness of the cladding showing the definitions of the maximum, average, and minimum strain failure criteria based on the equivalent plastic strain through the thickness of the remaining ligament of cladding (Note: $P_1 < P_2 < P_3$)

Using the criteria of the entire ligament reaching the critical necking strain of 11.2% may over predict the failure pressure since it does not account for some of the material thinning due to void growth in the ligament and the redistribution of stresses. Using the criteria of the first point reaching the critical strain may be too conservative. The average strain through the thickness may be a reasonable "best-estimate failure criterion", but using the 11.2% strain value from the uniaxial test is too high due to the biaxial condition.

Consequently in our work we provided the plots using the average strain through the ligament (for both 5.5% or 11.2% strain values), and to assess the differences with the SIA approach we also determined the pressure when the entire ligament exceeded the critical strain values of 5.5% or 11.2% strain.

Critical Strain Location

The "critical strain" region could be in the central region of the cladding or along the edge. The support conditions along the edge may highly influence the strain at that location. The precise edge conditions are unknown at this time, so a straight segment transition from the cladding-head interface to the outer surface of the head was assumed, as shown in Figure 5. Note that the recent SIA report showed the critical location was along the edge, where it was assumed the head thickness was a linear change from the clad-only region to a contour of the head thickness being equal to 75-percent of the design thickness. This corresponds to a thickness slope of 70 to 78 degrees in the SIA model, whereas in our model the slope varies from 35 to 65 degrees. Hence, the edge effects may be less severe in our model. In fact, in all our analyses with different cladding thicknesses and diameters, there was a change from the critical location when either the corrosion-hole diameter was larger or the thickness was smaller. There was a hole diameter to cladding thickness ratio where this occurs. It is recommended that the edge geometry should be documented when the corroded area is removed from the head and examined in a hot-cell.

Other Considerations in the "Failure Criterion"

In the analyses results presented in this report, the thickness in the cladding was a constant value, rather than using the variable thickness that occurs in welded cladding. Necking should start in the thinnest region, but the magnitude of the rupture area in the variable thickness case may be less than if the entire cladding had the minimum thickness.

Since the analysis conducted in this evaluation involved an axisymmetric assumption, the effect of an adjacent nozzle was not included. Engineering judgment suggests the nozzle may not be that important to the results, but the more detailed analyses to be done by ORNL may confirm that assumption.

The analysis in this report assumed that the corroded hole was perfectly circular. This of course is not the exact corroded area geometry; however, past corrosion research in the oil and gas industry suggests that there is little effect of the non-primary stress direction on the failure pressure[7]. Since the primary membrane loads are equal in a spherical head, the circular-hole geometry is the worst-case assumption for a limit-load analysis. The diameter in our analysis should correspond to the largest meridianal dimension in the actual corroded area.

This analysis did not account for any weld defects that may lower the "failure pressure". Such defects may give rise to a local necking region, and it is possible that a smaller leakage area may result if failure occurred at a cladding flaw.

[7] D. Stephens and B. Leis, "Development of an Alternative Criterion for Residual Strength of Corrosion Defects in Moderate- to High-Toughness Pipe", Proceedings of 2000 International Pipeline Conference, Vol. 2, pp. 781-792, October 2000.

FINITE ELEMENT ANALYSIS PROCEDURES

For the Davis-Besse head analysis conducted in this report, the corrosion defect was modeled as an axisymmetric pit at the center of the head. The effects of the irregular shape defect and presence of the control-rod penetrations were not included. The ABAQUS commercial finite element analysis software was used with four-noded axisymmetric elements. Figure 6 shows the detailed finite element mesh

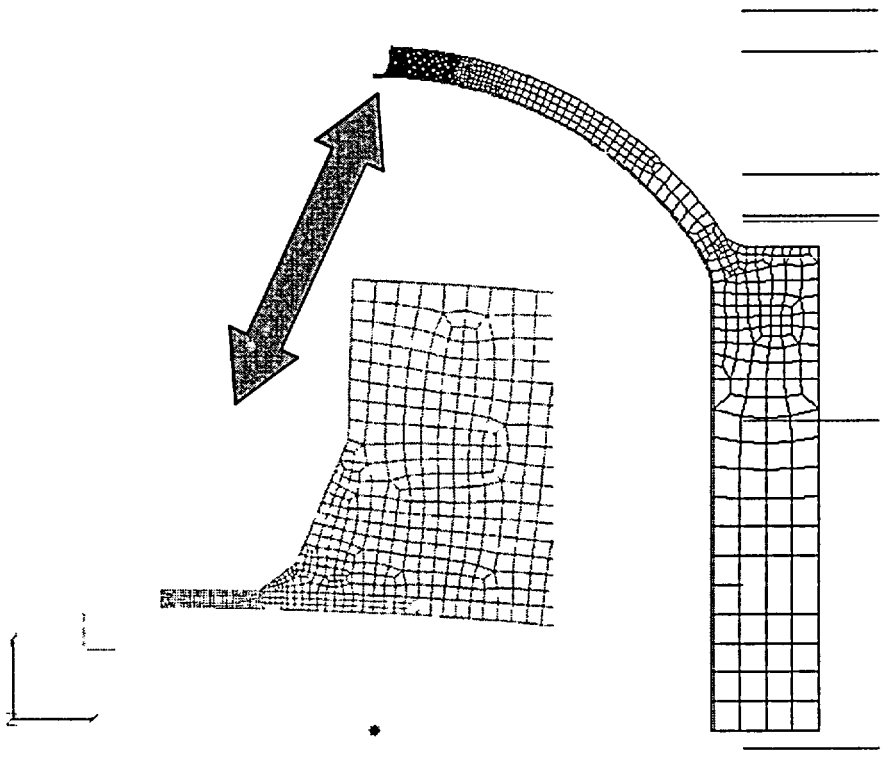

Figure 6 Axisymmetric finite element mesh for the Davis-Besse head

The dimensions of the Davis-Besse head used in these analyses were taken from detailed drawing supplied with the FirstEnergy's submittal to NRC bulletin 2001-01 (Docket Number 50-346). Four or five elements were used through the cladding thickness at the center location and 6 to 7 elements at the transition point from the cladding to the RPV head. The cladding thickness and the diameter of the corrosion hole were defined as variables. Large-strain analyses were conducted assuming incremental plasticity with isotropic hardening in the constitutive relationship. The detailed uniaxial stress-strain curve used for the cladding came from Framatome in response to a request from Emc^2, ORNL, and the NRC as is described in the previous section. An elastic-plastic stress-strain curve was used for the head material, but the stresses in the head material are generally elastic and have very little effect on the strains in the center of the cladding.

The stress-free temperature was 605F in these calculations. SIA used a stress-free temperature of room temperature, whereas the stress free temperature may be closer to 1,100F (the stress-relief temperature of the head after the cladding is put on). The cladding had a higher coefficient of thermal expansion than the low alloy steel head. Hence, using the stress-free temperature of 70F and taking the head to 605F produces a compressive stress in the cladding (SIA approach), our analysis was stress-free, but the real

situation would have a small tension stress in the cladding at 605F. The strains corresponding to these thermal expansion stresses, however, are small compared to the large strains at failure being calculated (about 0.1 percent strain versus the 5.5 to 11.2 percent failure strain criteria). Therefore, the errors from these assumptions are probably small compared to the uncertainties in the failure criterion.
To investigate the effect of large-strain versus small-strain analysis options, finite element runs were made with both options. Figure 7 shows the pressure versus strain results for one of the 15 cases investigated. Interestingly, the pressures were consistently higher for the large-strain analysis than for the small-strain analysis. Typically, the opposite is true, but with this geometry, the bulging of the cladding is perhaps better modeled with the large-strain option. Since the large-strain option is the most accurate, it was used for the rest of the analysis results that are presented in this report.

A total of 15 finite element analyses were conducted to investigate the effects of corrosion defect size and remaining cladding thickness on the failure pressure of the RPV head. Table 2 shows the matrix of the finite element analyses conducted.

Table 2 Matrix of finite element analyses

	Corrosion defect diameter (inches)		
Thickness (inch)	4.0	5.0	6.0
0.375 (maximum design)	X	X	X
0.297 (average measured in corroded area)	X	X	X
0.240 (minimum measured in corroded area)	X	X	X
0.188 (nominal design thickness)	X	X	X
0.125 (minimum design thickness)	X	X	X

The finite element results were analyzed to determine the pressure corresponding to the equivalent plastic strain in the ligament. The model idealized the corrosion as a circular region with the remaining cladding layer having a constant thickness. No attempts were made to analyze the precise transition from the cladding layer to the remaining head material at the perimeter of the defect region since that information is not know at this time. Rather, the transition in the wall thickness from the cladding to the full head thickness was made so that it was believed to be somewhat realistic of a gradual change rather than assuming an instantaneous change in thickness. It is expected that the ORNL 3-D analyses will attempt to model the edge effects in detail when they become available. As a result, for a given loading increment, the maximum plastic strain in the cladding layer occurred at the center of the axisymmetric model used in the analysis in this report. At each loading increment, the maximum, minimum, and average values of the equivalent plastic strain through the ligament were recorded. Figure 7 shows a typical plot of the strain at the center of the cladding versus pressure for the case of a 5-inch diameter defect with a cladding thickness of 0.297 inch. Plots similar to Figure 7 for each of the 15 finite element analyses are given in Appendix A for the large-strain analyses. The small-strain analyses results are given in Appendix B, but were not used further in this report.

The summary plots shown in the next section show the diameter of the head corrosion versus pressure for a given thickness at strains of either 5.5% or 11.2% using the minimum, maximum, and average strains through the thickness criteria. We believe the 5.5% strain limit as an average value through the thickness may be the best estimate of the actual failure pressures.

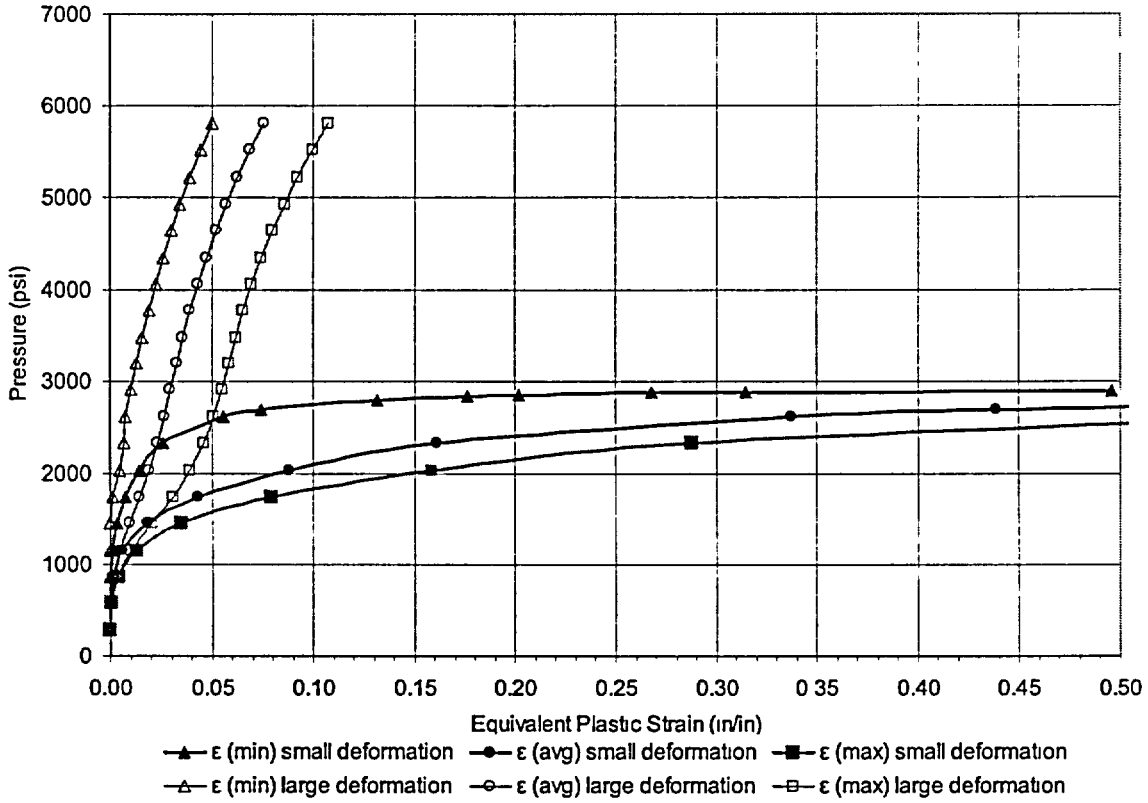

Figure 7 Plot of equivalent plastic strain at center of cladding versus internal pressure for both small-deformation and large-deformation analyses for a 6-inch diameter corrosion area and a cladding thickness of 0.297 inch

RESULTS OF PARAMETRIC STUDY SHOWING "FAILURE PRESSURE" VERSUS CORRODED AREA

In order to simplify the numerous pressure versus strain plots that are given in Appendix A, the pressure as a function of corrosion diameter corresponding to the maximum, the minimum, and the average strain in the cladding layer for both the 5.5% and 11.2% strain levels were determined. Recall that the 5.5% strain criterion was determined by considering the effect of biaxial loading on the stress-strain curve up to the same uniaxial ultimate stress value. No efforts could be made at this time to estimate if necking would occur at a lower stress value due to the higher triaxial stress conditions in the actual structure than in a uniaxial tensile test. Experimental data or more detailed analyses are needed to make that determination. Results of the critical strain being reached either in the center of the cladding or at the edge were investigated. First the center cladding location results are given in detail and reduced to the key figure. For the edge location, the detailed plots are given in Appendix A, and only the key figure is given. A comparison of the two plots for determining a calculated "failure pressure" is given afterwards.

Results at Center of Clad-only Region

The following plots show "failure pressure" versus the diameter of the corroded area for a given thickness of cladding. The "failure pressure" represents the internal pressure corresponding to the equivalent plastic strain in the center of the cladding layer previously described.

Figure 8 through Figure 12 show the diameter of the head corrosion versus "failure pressure" for each of the following five values of cladding thickness;

- 0.375" – maximum design cladding thickness,
- 0.297" – average thickness of the cladding measured by the utility,
- 0.240" – minimum thickness of the cladding measured by the utility,
- 0.188" – average design cladding thickness, and
- 0.125" – minimum design cladding thickness.
-

Note: the pressure values in the following figures were estimated graphically from the plots given in Appendix A.

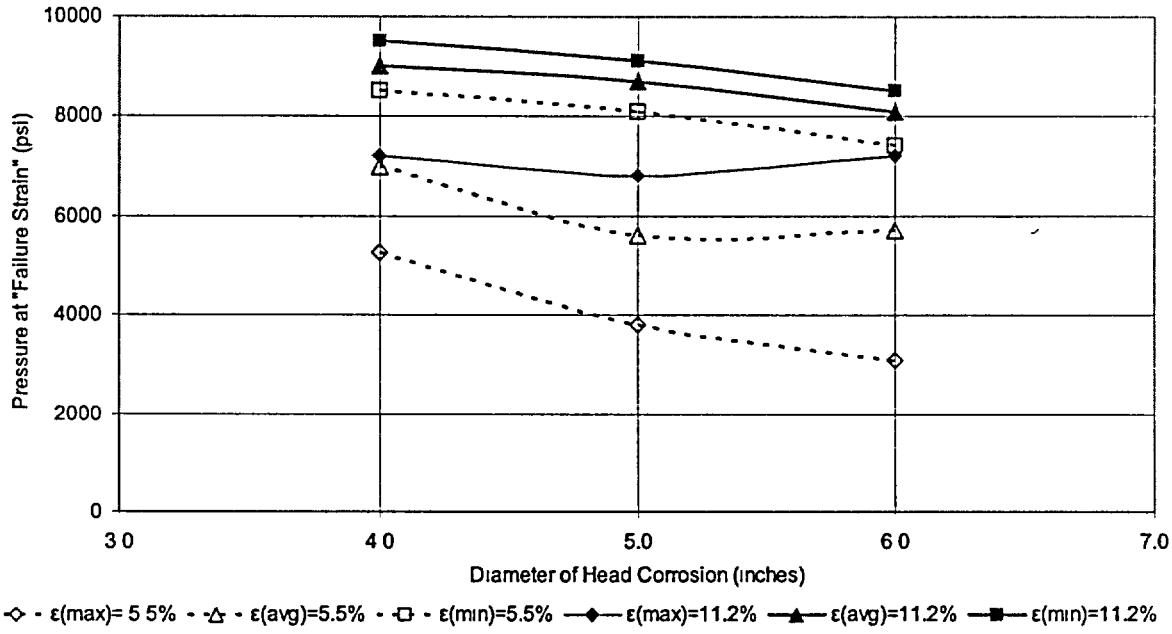

Figure 8 Corrosion diameter versus "failure pressure" for critical strain at center of cladding for cladding thickness of 0.375 inch

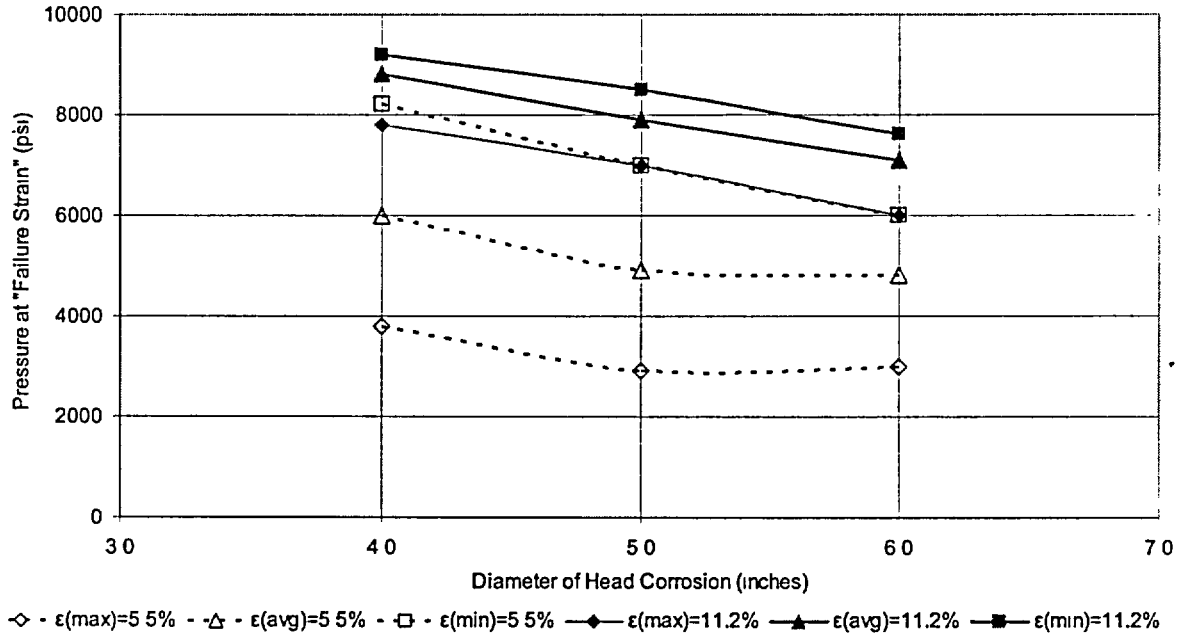

Figure 9 Corrosion diameter versus "failure pressure" for critical strain at center of cladding for cladding thickness of 0.297 inch

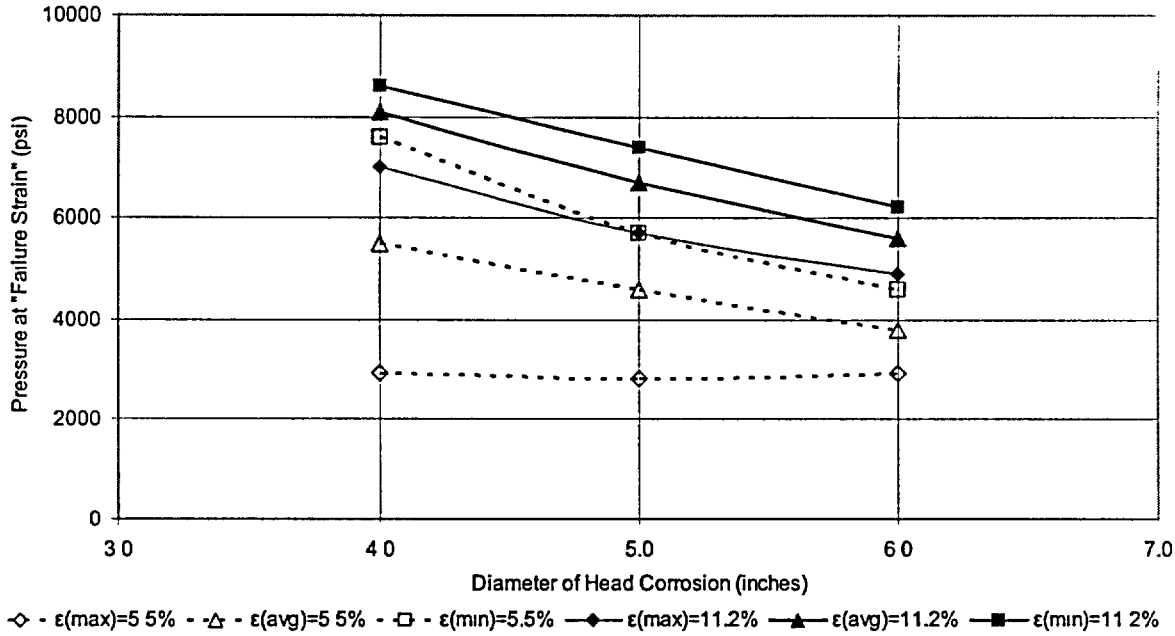

Figure 10 Corrosion diameter versus "failure pressure" for critical strain at center of cladding for cladding thickness of 0.240 inch

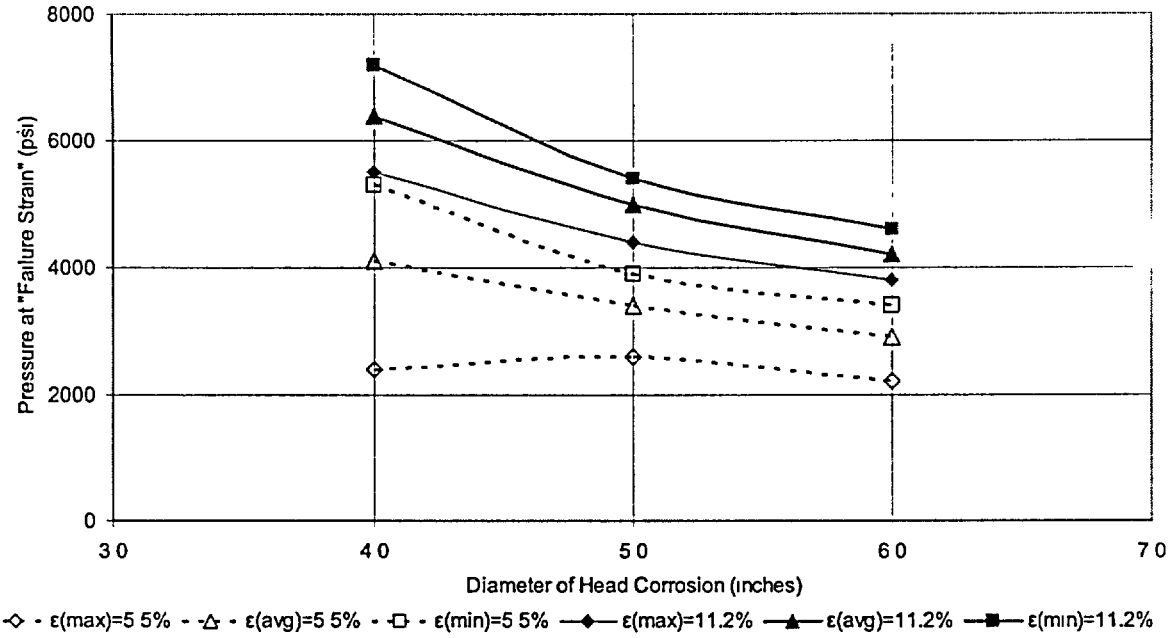

Figure 11 Corrosion diameter versus "failure pressure" for critical strain at center of cladding for cladding thickness of 0.188 inch

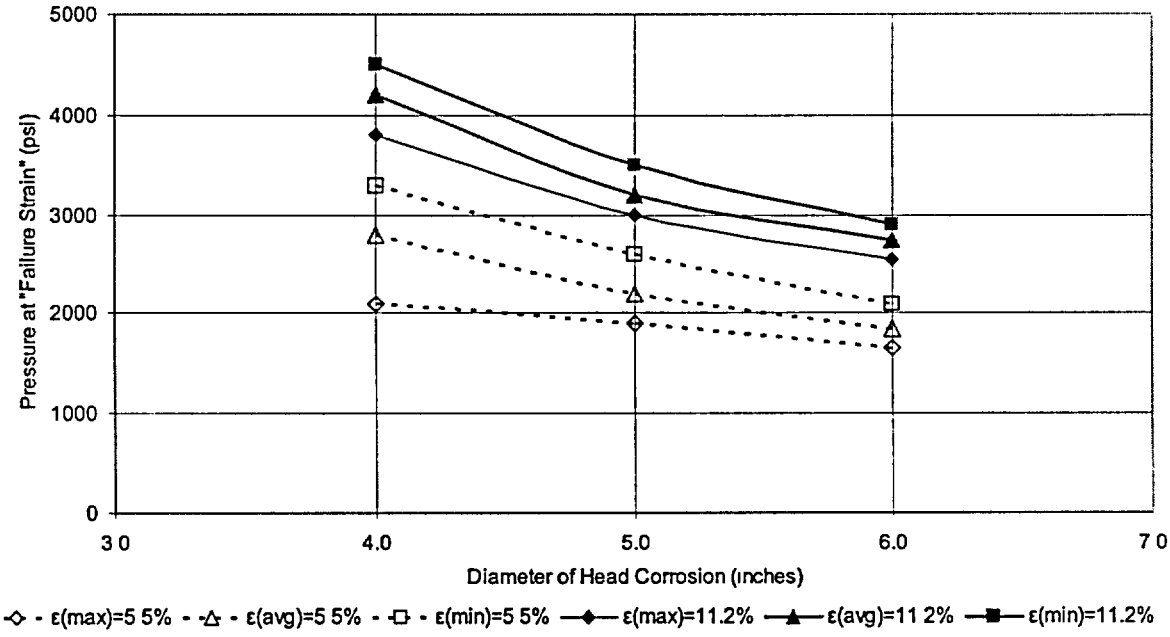

Figure 12 Corrosion diameter versus "failure pressure" for critical strain at center of cladding for cladding thickness of 0.125 inch

Another way to assess this data is to plot the "failure pressure" versus cladding thickness for a given diameter of corrosion. One plot of this type is shown in Figure 13 for illustration purposes.

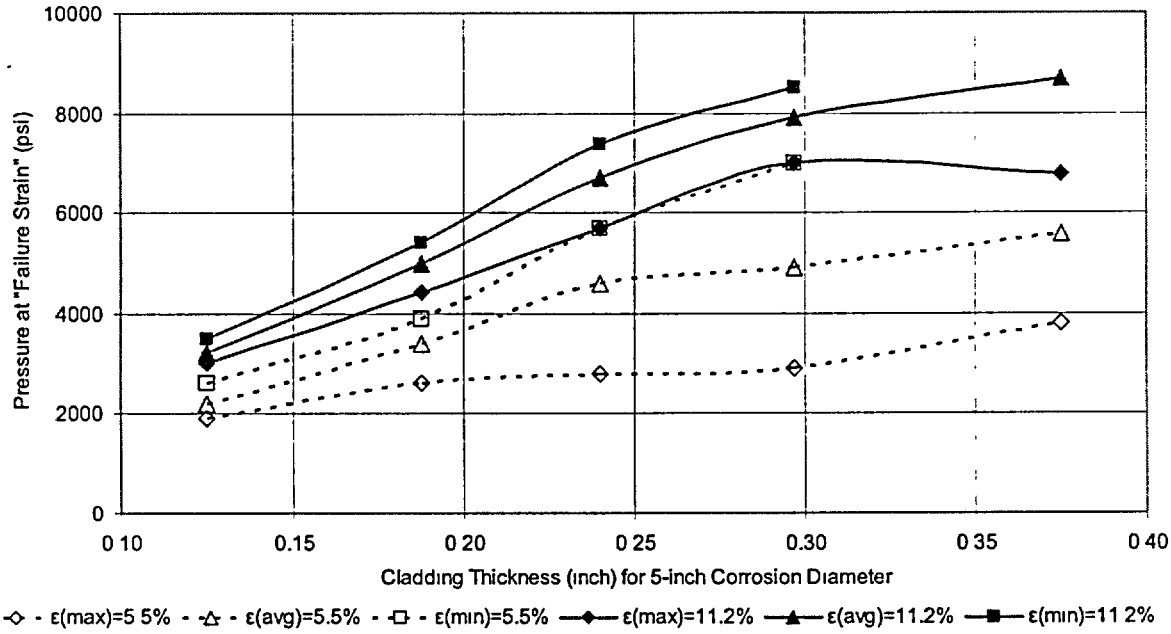

Figure 13 Cladding thickness versus "failure pressure" for critical strain at center of cladding for 5-inch diameter corrosion area

Values from Figure 9 through Figure 12 have been combined by normalizing the corrosion diameter with respect to the ligament thickness and plotting the results versus "failure pressure" for having the strain in the center of the cladding. Plots of pressure versus D/t are shown in Figure 14 and Figure 15 for the critical strains of 5.5% and 11.2%, respectively. The three different strain gradient criteria are shown in each figure. These figures show that the data from the pressure-versus-diameter plots for each thickness collapse to a single curve for a given failure criterion. The first occurrence curves are believed to give too low of "failure pressure", whereas the average strain curves are believed to give a best estimate of the expected failure pressure. Hence, Figure 14 and Figure 15 can be used to calculate the "failure pressure" for a significant range of corrosion diameters and thicknesses of interest.

Figure 16 shows a comparison of the 5.5% average-failure-strain criterion (Emc^2 best-estimate failure criterion) to the 11.2% minimum-failure-strain criterion (SIA criterion).

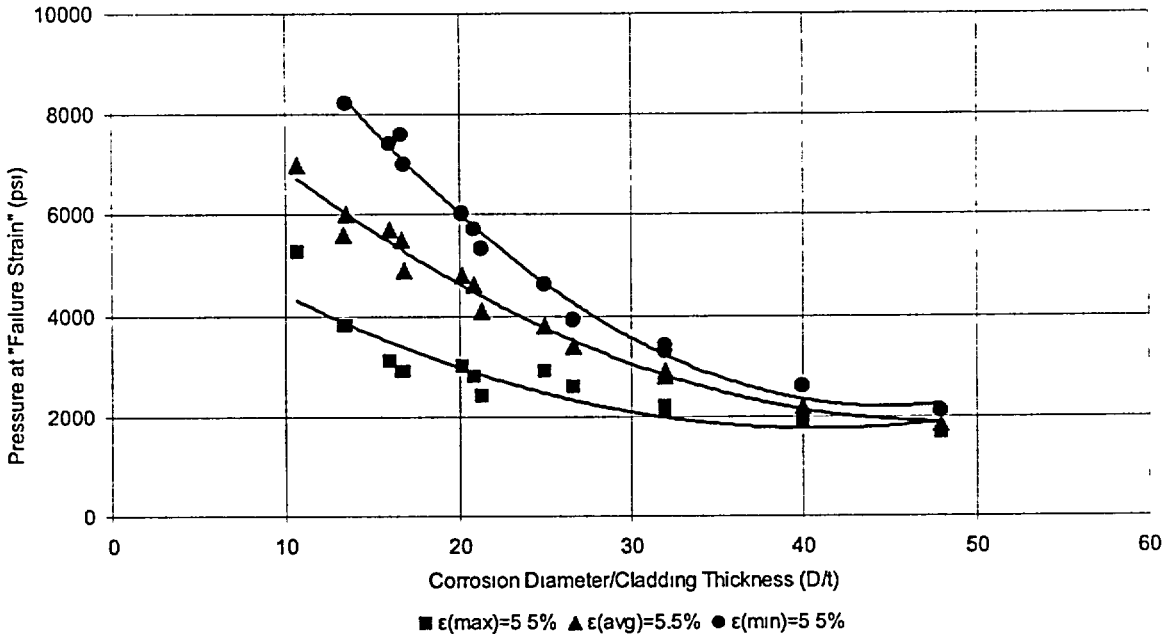

Figure 14 Plot of D/t versus failure pressure for the 5.5% strain criterion in the center of the cladding

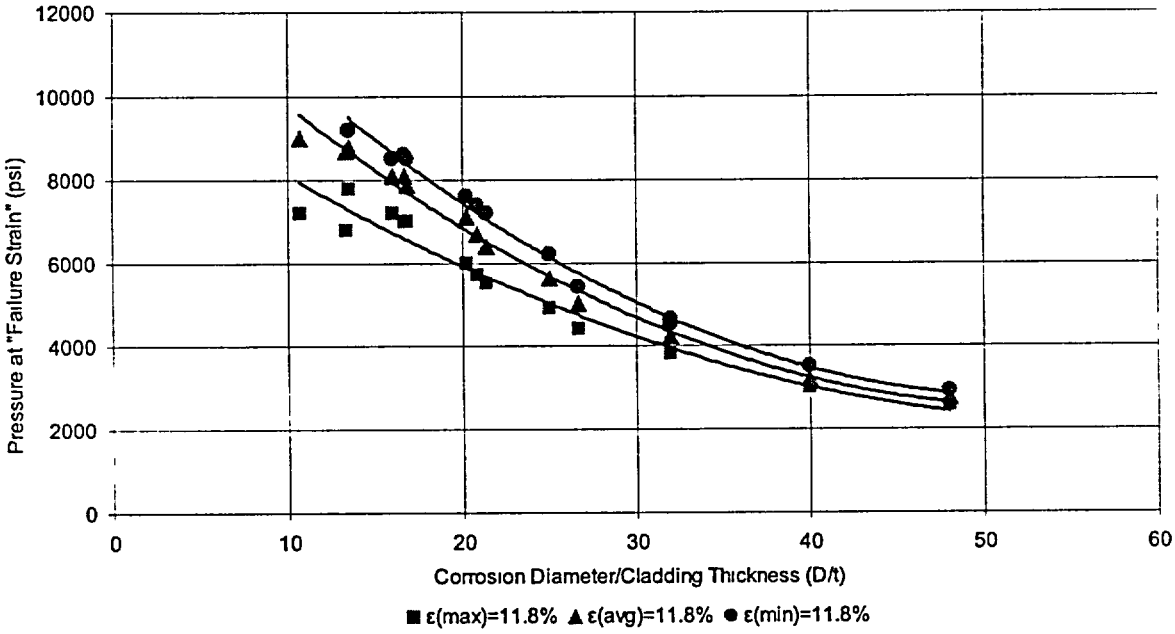

Figure 15 Plot of D/t versus pressure for the 11.2% strain criterion in the center of the cladding

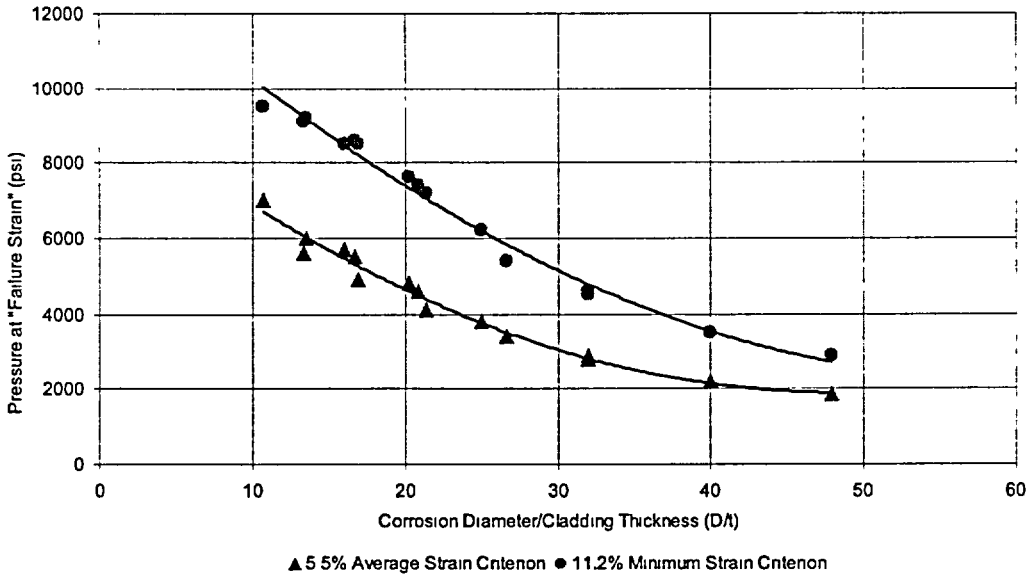

Figure 16 Plot of D/t versus pressure for comparing the 5.5% average failure strain criterion to the 11.2% minimum failure strain criterion at center of cladding

Figure 17 shows the ratio of the failure pressures for the 11.2% minimum strain criterion at the center of the cladding (SIA failure criterion) to the 5.5% average strain criterion (Emc^2 best-estimate failure criterion) as a function of corrosion diameter to cladding thickness, D/t. The figure shows that the failure pressure using the 11.2% minimum strain criterion exceeds that of the 5.5% average strain criterion by approximately 60% over the range of D/t investigated.

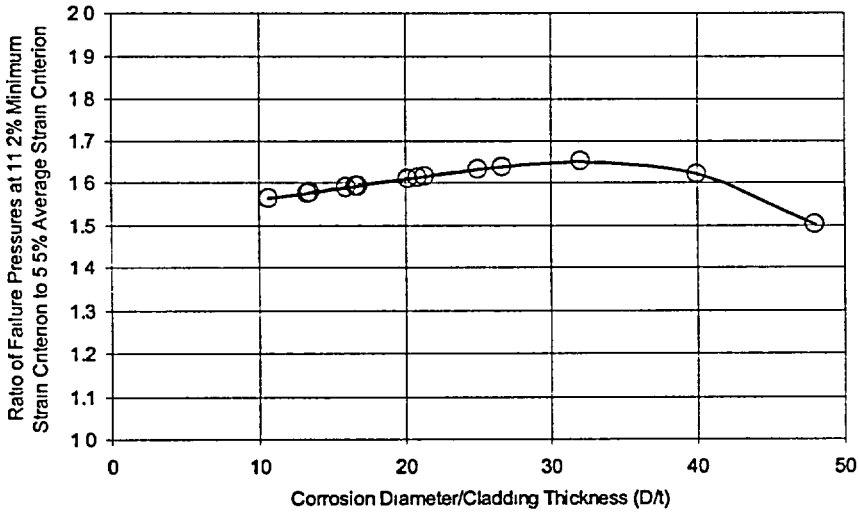

Figure 17 Ratio of the "failure pressures" from 11.2% minimum strain criterion used by SIA to the Emc^2 best-estimate 5.5% average strain criterion as a function of corrosion diameter to cladding thickness (D/t) at center of cladding

Edge Location Results

The other critical strain location could be along the edge or perimeter of the hole. This result may be dependant on the geometry of the transition of the cladding thickness to the head thickness. Figure 5 showed the geometry used in our analyses, whereas the edge geometry in the SIA case was a simple linear slope of about 70 to 78 degrees at the critical edge location, and ORNL used a 90 degree thickness transition.

The details of all the edge-location pressure versus strain plots are given in Appendix A. Rather than recreate similar figures to Figures 8 through 16, only a figure similar to Figure 16 is given here to summarize all the results from the edge-location "failure pressure" versus dimensionless hole geometry (diameter of the hole over the cladding thickness, D/t). These results are shown in Figure 18 for the Emc^2 "best estimate failure criterion" (5.5-percent average strain through thickness) and the failure criterion used in the SIA report (11.2 percent strain exceeded throughout the thickness).

Figure 19 shows a comparison of the center and edge "failure pressures" versus dimensionless hole geometry. Interestingly, there is a transition of the critical location from the center of the cladding to the edge of the cladding when the hole diameter to cladding thickness ratio (D/t) is 12 for the 5.5-percent average strain criterion. For the 11.2-percent minimum strain criterion, the center region had a slightly lower "failure pressure" than the edge location for all D/t values.

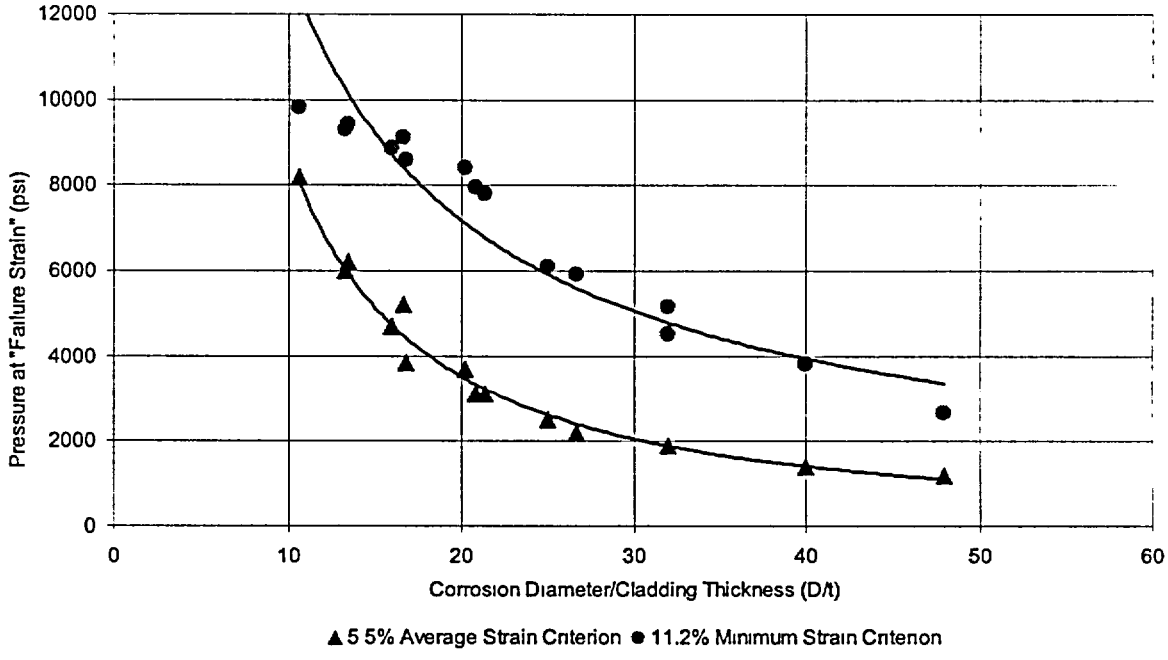

Figure 18 Plot of D/t versus pressure for comparing the 5.5% average failure strain criterion to the 11.2% minimum failure strain criterion at edge of cladding

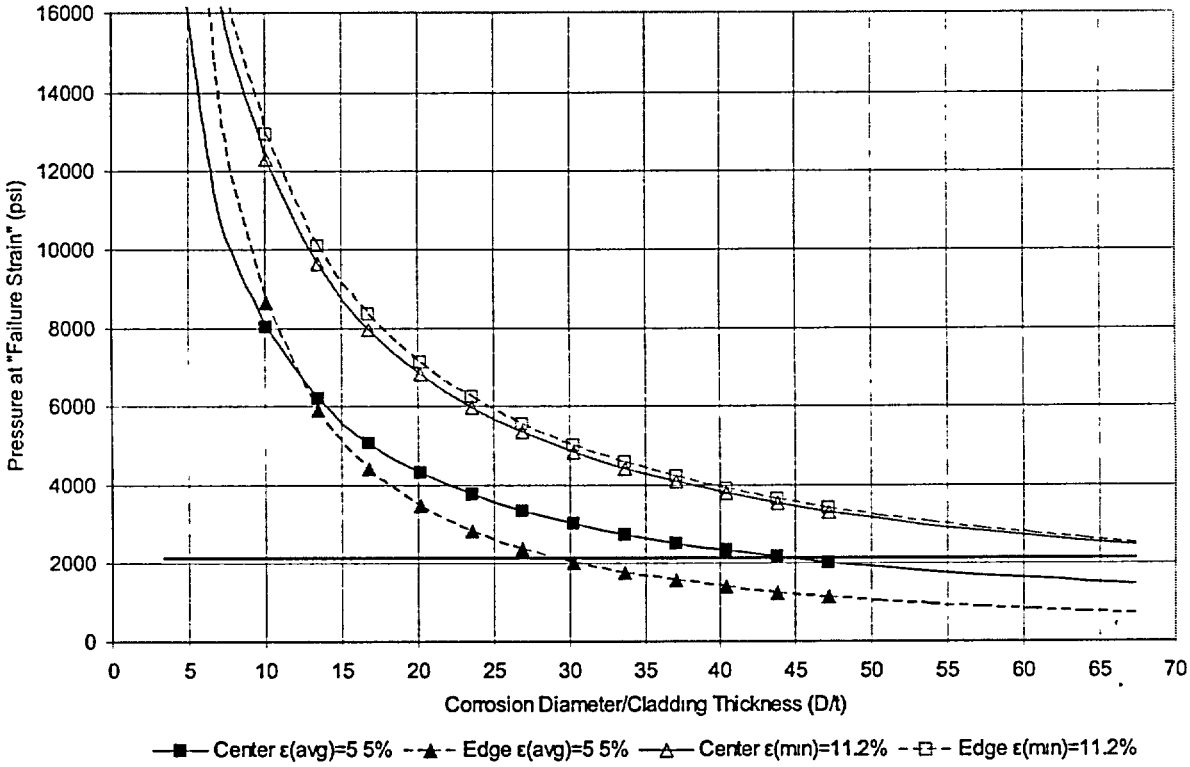

Figure 19 Comparison of "failure pressures" versus D/t for center and edge locations

Calculated Margins

To determine the margins on either the failure pressure or the margin on the hole diameter, it is first necessary to characterize the corrosion area in terms of an equivalent diameter. Figure 20 shows the remaining thickness measured on the RPV head between Nozzles 3 and 11. These measurements were taken at a spacing of approximately one square inch by Davis-Besse and their contractors. While these were preliminary measurements, the figure shows that the minimum thickness of 0.240 inch was measured at one location. In addition, there is a region between the nozzle openings where the thickness is less than 0.300 inch over an irregular area. The longest continuous segment in which the cladding thickness does not exceed 0.300 inch is approximately 6.7 inches, as shown by the solid line, or 7.6 inches as shown by the dashed line where only one reading was greater than 0.300 inch in Figure 20.

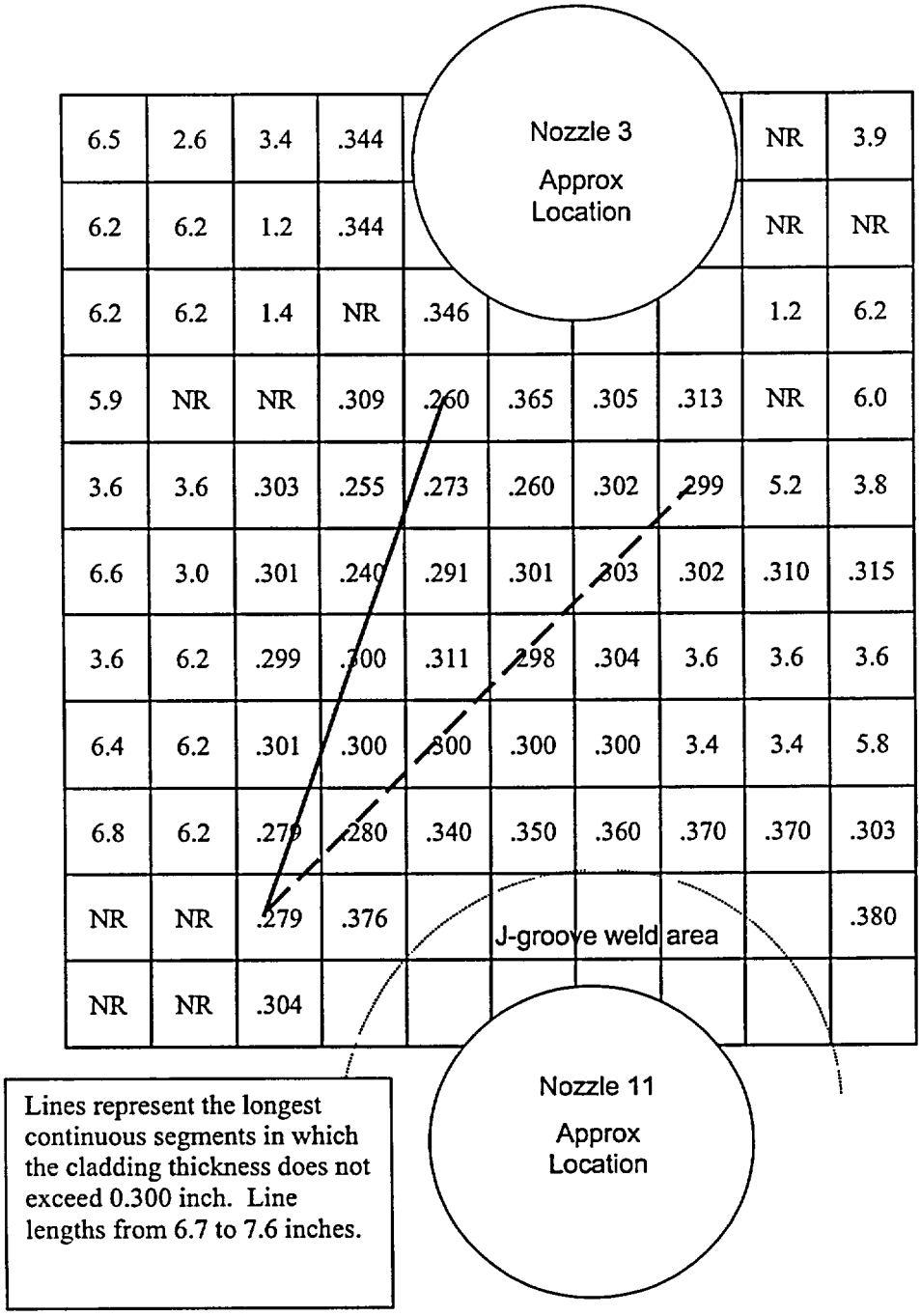

Figure 20 Layout of the remaining thickness measurements between nozzles 3 and 11 of the RPV head

Margins on Failure Pressures

The fit through the finite element results shown in Figure 19 was used to make a plot of the bounding failure pressure versus hole diameter for a cladding thickness of 0.297 inch. The results are shown in Figure 21 for corrosion defect diameters up to 20 inches. The symbols in Figure 21 indicate were FE results were available. The solid line beyond the symbols is an extrapolated curve-fit equation. A nominal operating pressure of 2,155 psi is also indicated in the figure.

Assuming that the shape of the corrosion defect has less affect on the failure pressure than the largest meridianal dimension (from gas pipeline corrosion experience), then using the approximate meridianal dimensions of 6.7 to 7.6 inches (from Figure 20) gives a "best-estimate failure pressure" range of 3,000 to 2,300 psig, respectively. This gives a margin on the operating pressure of 1.39 to 1.07, respectively. Both of these failure predictions are for the edge location, where the actual geometry used is not well known at this time.

Using these same dimensions with the minimum-strain failure criterion with 11.2% critical strain (SIA criterion), the calculated failure pressure would be about 6,300 to 5,700 psig, respectively. This gives a margin of 2.92 to 2.65, respectively.

The ratio of the failure pressures from the two criteria is roughly the factor of 2.2. This is greater than the 1.6 value from Figure 17 since the 5.5% strain criterion has the critical location at the edge of the hole not at the center.

Margins on Corrosion Cavity Diameter

Another estimate that could be made from Figure 21 is the size of the corrosion area that could cause failure at the normal operating pressure. Using the average strain criterion with 5.5-percent critical strain gives a meridianal length (diameter from Figure 21) of approximately 8.5 inches, or 0.9 to 1.8 inches of additional corrosion length. Using the SIA minimum-strain failure criterion with 11.2-percent strain gives a meridianal length of approximately 23 inches (extrapolated from Figure 21), or 15.3 to 16.3 inches of additional corrosion for failure at the operating pressure.

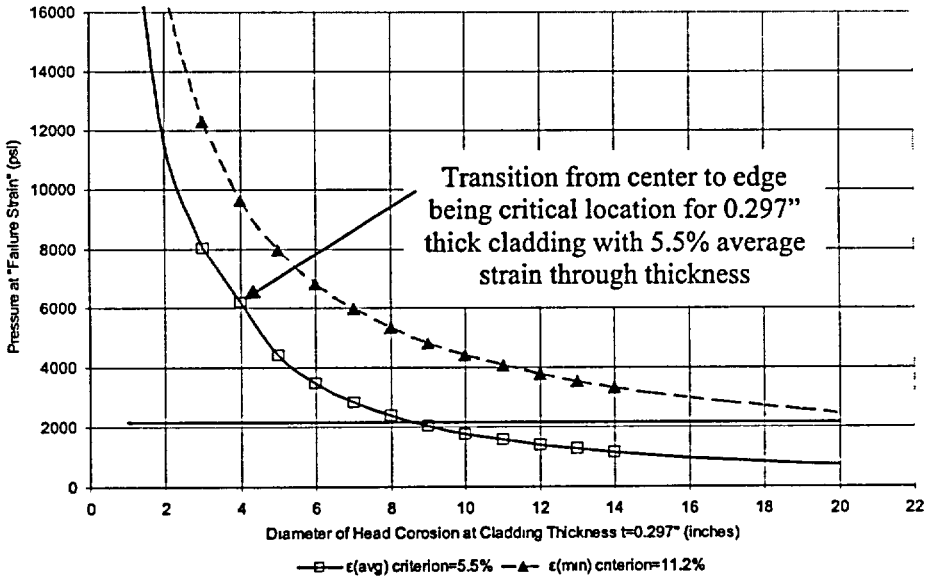

Figure 21 Extrapolated curve-fit of FE values for a cladding thickness of 0.297 inch

DISCUSSION

The results in this evaluation showed that the failure criterion is a significant factor in determining the calculated "failure pressure". The values given in the previous section were meant to be an approximate bounding of the "failure pressures" given the lack of definite geometry of the cladding to head transition, the lack of validation of the failure criterion, and the axisymmetric assumption in the analyses. The Emc^2 values came from models where the edge geometry (see Figure 5) was such that the critical strain region occurred at the edge of the cladding.

To get better confidence in the values calculated, comparisons were also made between the Emc^2, SIA, and preliminary ORNL results. Table 3 summarized the calculated "failure pressures" that are discussed below, including the calculated "failure pressure" margins on the operating pressure and the maximum transient pressure of 2,750 psig.

The SIA report gives a calculated "failure pressure" of 5,600 psig for the 0.297-inch average thickness. This analysis used the 11.15-percent strain criterion with the strain having to occur completely through the thickness. This pressure corresponded to their pressure increment just prior to reaching that strain value completely through the thickness. The maximum strain they reported was 44.56 percent strain and the average value through the thickness was 23.9 percent strain. Using the SIA failure criterion, the results in this report give calculated "failure pressures" of 5,700 to 6,300 psi. The SIA analysis also predicted the critical strain location to be at the edge of the hole.

SIA did not supply pressure versus strain plots in their report to assess what "failure pressure" they would have calculated if they used the Emc^2 failure criterion of the 5.5-percent strain occurring as an average value through the thickness. However, using the factor of 2.2 from the analysis trends in this report allows an estimate to be made of what their failure strain would have been with the Emc^2 criterion. That "failure pressure" would have been 2,545 psig, which is between the Emc^2 values of 2,300 and 3,000 psig given in the previous section.

Preliminary results were also available from ORNL[8]. They calculated pressure versus strain values at the center of the clad-only area and at the edge of the cladding. Although their work is ongoing at this time, an initial estimate is that the "failure pressure" with the 5.5 percent average strain criterion was approximately 3,680 psig. At the edge of the hole, their pressure corresponding to an average strain of 5.5 percent through the thickness was approximately 3,950 psig. Hence, with the edge conditions in their model the center cladding area was the critical location.

Table 3 Summary of calculated "failure pressures" using criterion of 5.5-percent average strain through the thickness (using average thickness of 0.297 inch)

	"Failure pressure", psig	Margin on operating pressure	Margin on upset pressure of 2,750 psig
Emc^2 *	2,300 to 3,000	1.07 to 1.39	0.87 to 1.09
SIA**	2,545	1.18	0.92
ORNL – preliminary***	3,680	1.71	1.34

* Based on meridianal lengths of 6.7 to 7.6 inches.

** Estimated using factor of 2.2 for different failure criterion from trends in this report.

*** Averaging their strain values through the thickness from their preliminary analyses.

[8] P. T. Williams and B. R. Bass, "Analysis of Davis Besse RPV Head with Detailed Submodel of Wastage Area," Preliminary report to NRC, April 30, 2002.

The relatively good agreement between the Emc^2 and modified SIA results (when using the same failure criterion) predicted the critical location as being at the edge of the cladding region. The higher preliminary ORNL results have the failure at the center of the cladding. Additional refinement of the mesh in the ORNL analysis is underway to explore this.

CONCLUSIONS

The efforts conducted in this report involved making a best-estimate evaluation to determine the margins on the calculated "failure pressure" to operating pressure and how much additional corrosion might be needed to cause failure at the operating pressure for the Davis-Besse RPV head corrosion case. The conclusions from this investigation were:

1. The uniaxial stress-strain curve at 600F supplied by Framatome from the *Nuclear Systems Materials Handbook* was compared to stress-strain curves for TP308 weld metal at 550F from the PIFRAC database and was found to be more representative of the average stress-strain curve from the PIFRAC database rather than a minimum value. The material documented in the PIFRAC database was not stress relieved, and it is not known if the *Nuclear Systems Materials Handbook* material was stress relieved. The cladding on the head was stress relieved. Stress relieving may slightly reduce the stress-strain curve.

2. The uniaxial stress-strain curve can be used to calculate the strain at the same ultimate stress value for biaxial loading. This involves a relatively fundamental use of Hook's Law, Von Mises equation, and the Distortion Energy Theorem. The resulting strain under biaxial loading was about half of the uniaxial strain for the TP308 weld metal; i.e., 5.5-percent strain, rather than 11.2 percent strain. This result is consistent with engineering judgment for several metallurgist, and university professors that deal with metal-forming-limit diagrams for biaxial loading in the automotive and shipbuilding industries. An analysis by McClintock on failure stress for a sphere under pressure loading (pure biaxial membrane loading) gave a similar trend for pure 1:1 biaxial loading.

3. Fifteen axisymmetric finite element analyses were conducted with large-strain assumptions. The pressures corresponding to the equivalent strains were calculated for a variety of cladding thicknesses and cavity diameters. The strains varied through the thickness of the cladding, so pressures corresponding to three possible failure criteria were calculated:
    a. The pressure when the cladding strain was first reached the critical strain,
    b. The pressure when the average strain through the thickness of the cladding reached the critical strain, and
    c. The pressure when the strain in the entire thickness of the cladding exceeded the critical strain.

    It was felt that Criterion (a) would be too conservative, Criterion (b) was a reasonable best estimate in the absence of experimental data or further detailed analyses, and Criterion (c) would overestimate the failure pressure.

4. The location of the "critical strain" could be at either the central region of the cladding or along the edge. The precise edge support geometry (how the head corroded close to the cladding) is not well known at this time, so a straight segment approximation of the transition was used in the models. With this edge condition, the critical strain location was at the edge of the clad-only region in our analysis. This was consistent with the SIA results.

5. For a given failure criterion (strain location, strain level, and strain distribution through the thickness) the finite element analyses for the various thickness and hole diameters could be expressed in a normalized graph of pressure versus D/t where "D" is the maximum diameter or length of the corrosion area, and "t" is the thickness of the cladding. This allowed the results from these analyses to be extrapolated to greater diameters than actually run.

6 From experience in corroded pipe analyses for the gas pipeline industry, the critical dimension in the actual corroded cavity is probably the maximum meridianal length where the cladding thickness remained at a minimum value. This length was between 6.7 and 7.6 inches.

7. The calculated failure pressure using the best-estimate criterion (average strain in the ligament reaching the biaxial strain limit of 5.5 percent) resulted in a calculated "failure pressure" of 3,000 to 2,300 psig for the 6.7 to 7.6 inch lengths, respectively. This is a margin of 1.07 to 1.39 at the operating pressure, or 0.87 to 1.09 at a transient pressure of 2,750 psig, i.e., failure was predicted to occur at the transient pressure.

8. The ratio of the calculated pressure from the "failure criterion" with either the equivalent strain at 11.2 percent occurring completely through the thickness (as used in the SIA report) or 5.5 percent average strain through the thickness (Emc^2 "best-estimated failure criterion") was a factor of approximately 2.2.

9. The margin on the maximum dimension of the corroded cavity at the operating pressure was also determined. Using the "best estimate criterion", the cavity would have to increase in the longest direction by 0.9 to 1.8 inches.

10. Comparisons were made with the calculated "failure pressures" from this analysis, the SIA analysis, and preliminary analyses from ORNL. The SIA "failure pressures" were reduced by the factor of 2.2 to account for the "best-estimate failure criterion". The SIA margin on the operating pressure was then determined to be 1.18, which is bounded by the 1.07 to 1.39 values from this report. The ORNL preliminary results using the same criterion gave a value of 1.71, but their failure location was in the center of the cladding rather than the edge, and further mesh refinement is being explored.

11. These margins may be affected by several factors:
    a. Variable thicknesses, i.e., these margins were calculated using the average thickness of 0.297 inch, while there was a single measured location where the thickness was down to 0.24 inch. A calculation with a constant thickness of 0.24-inch thickness could be made, but it may be overly conservative in bounding the failure pressure.
    b. Flaws in the cladding could cause a local limit-load failure at a lower pressure, probably resulting in a smaller opening area than if the cladding failed without a flaw.
    c. There is the possibility that the 5.5 percent equivalent strain failure criterion (based on reaching the uniaxial ultimate strength under 1:1 biaxial loading) could be lower due to enhancement of void growth under higher triaxial stresses. Edge-loading conditions would give higher triaxial stresses than the center of the clad-only region.
    d. The assumption of using the average strain through the thickness to account for the current FE analysis inability to account for redistribution of stresses once the critical strain where void growth (necking) starts, is an important factor.
    e. A different slope of the transition from the cladding thickness to the full head thickness may affect the results from all analyses.
    f. The stress-strain curve appears to be an average curve rather than a minimum. The actual stress-strain curve of the clad material could increase or decrease the failure loads.

12. More detailed analyses for the ORNL efforts will be helpful in determining the margins estimated from the plastic displacement or bowing in the cladding that was measured in the Davis-Besse head once further refinement of the mesh is made.

13. The accuracy of the "failure criterion" may require some experimental data to determine the biaxial strain limit of the cladding material at the operating temperature. Alternatively, a FE analysis using Gurson elements in ABAQUS could be conducted if the proper parameters for the Gurson element can be determined for the cladding material (inclusion size and distribution [f_0 and D values from the Tvergaard and Hutchinson approach[9]]). Test data exist where those values could be independently determined and then applied to the unflawed (or even a flawed) cladding analysis.

14. It is recommended that once the corroded region is cut from the head and sent for evaluation, the geometry of the transition from the cladding layer to the outside surface of the RPV head be determined. A silicon mold of the cladding surface could be made to determine the variability of the thickness.

[9] C. F. Shih, L. Xian, and J. Hutchinson, "Validity Limits in J-Resistance Curve Determination – A Computational Approach to Ductile Crack Growth under Large-Scale Yielding Conditions," NUREG/CR-6264, Vol. 2, February 1995.

APPENDIX A

Plots of Equivalent Plastic Strain versus Pressure at the Center of the Cladding Area and at the Edge of the Cladding Layer and the Head for the Large Deformation Analyses

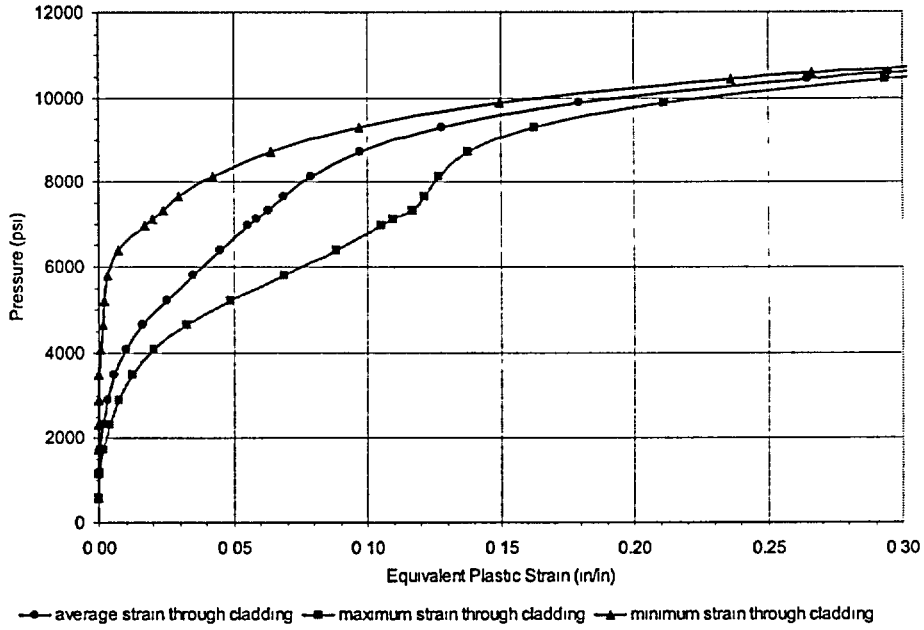

Figure A-1 Equivalent plastic strain versus pressure at the center for corrosion diameter of 4 inches and cladding thickness of 0.375 inch

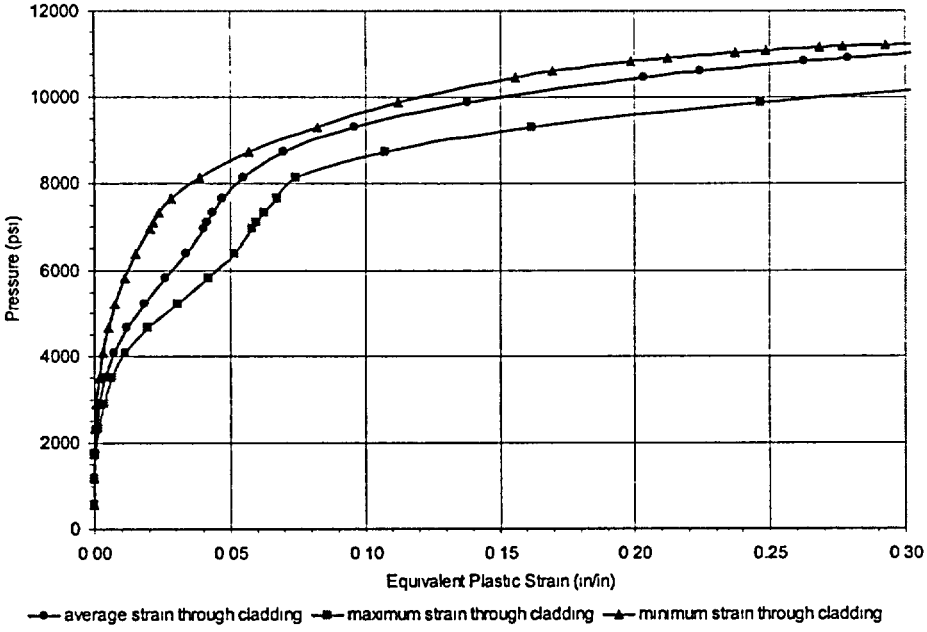

Figure A-2 Equivalent plastic strain versus pressure at the edge for corrosion diameter of 4 inches and cladding thickness of 0.375 inch

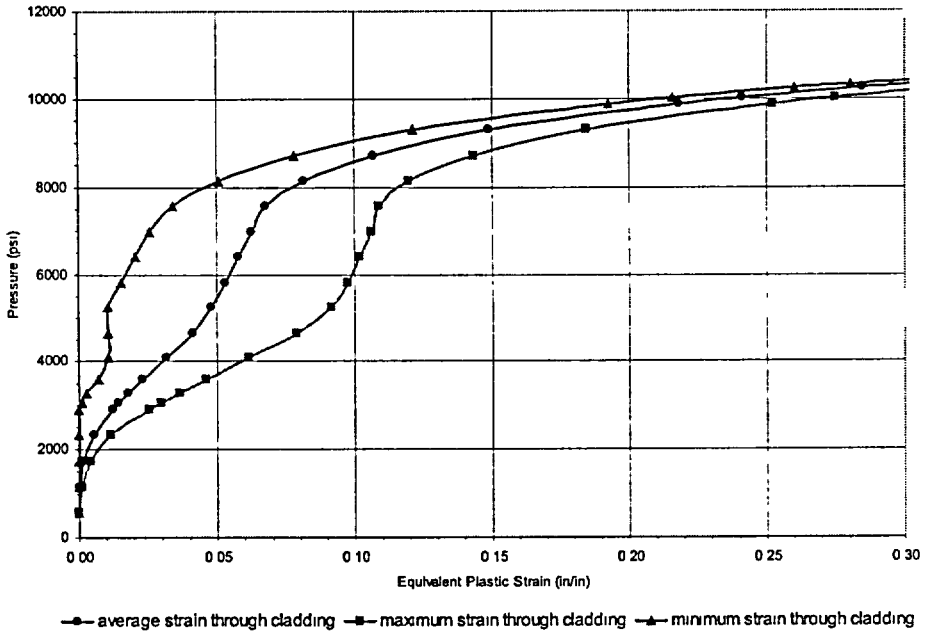

Figure A-3 Equivalent plastic strain versus pressure at the center for corrosion diameter of 4 inches and cladding thickness of 0.297 inch

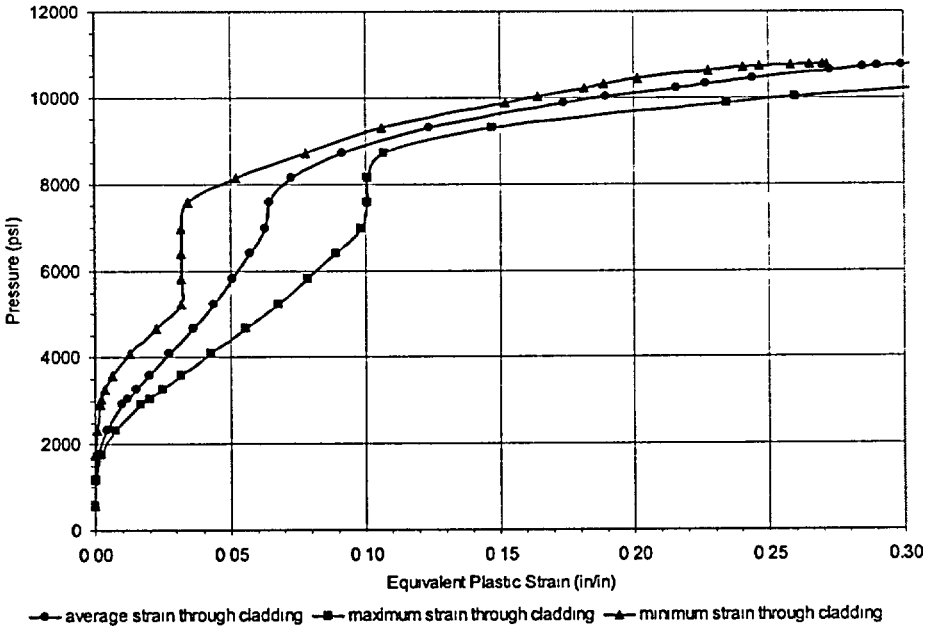

Figure A-4 Equivalent plastic strain versus pressure at the edge for corrosion diameter of 4 inches and cladding thickness of 0.297 inch

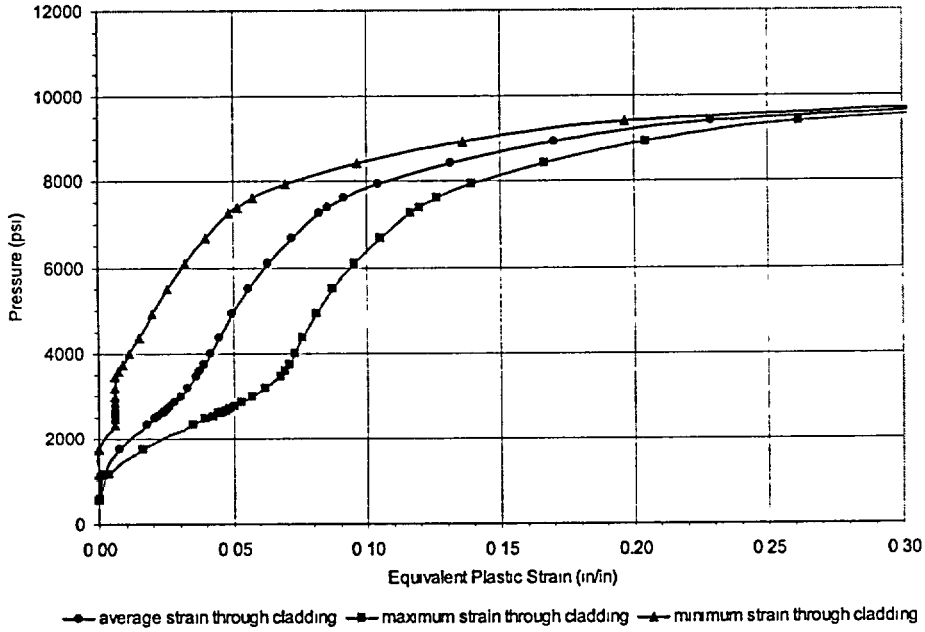

Figure A-5 Equivalent plastic strain versus pressure at the center for corrosion diameter of 4 inches and cladding thickness of 0.240 inch

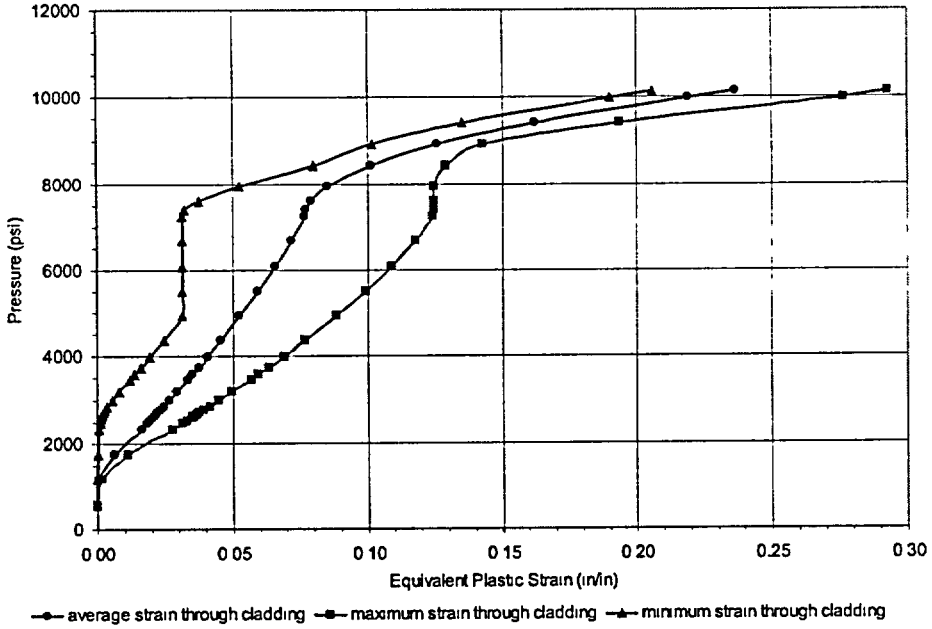

Figure A-6 Equivalent plastic strain versus pressure at the edge for corrosion diameter of 4 inches and cladding thickness of 0.240 inch

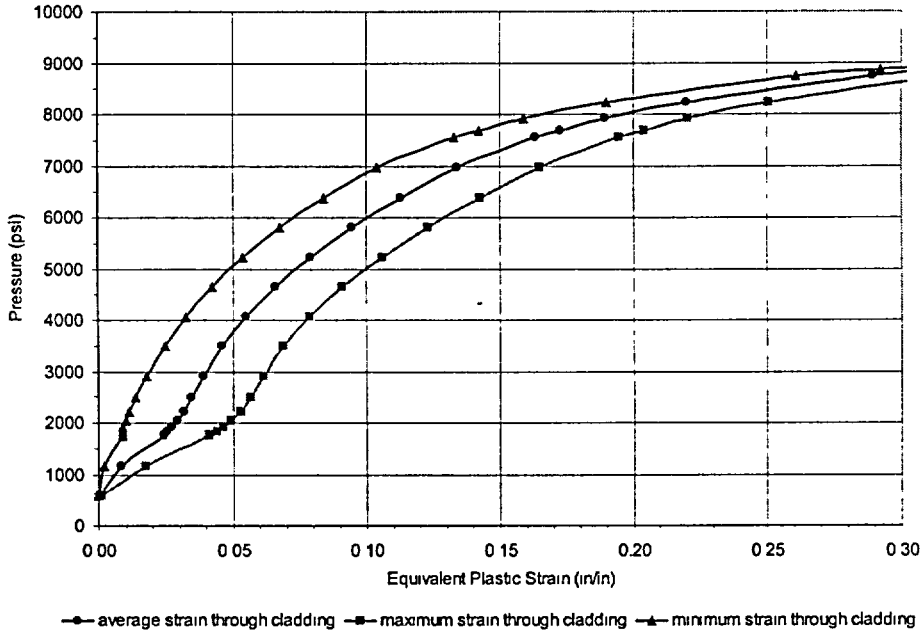

Figure A-7 Equivalent plastic strain versus pressure at the center for corrosion diameter of 4 inches and cladding thickness of 0.188 inch

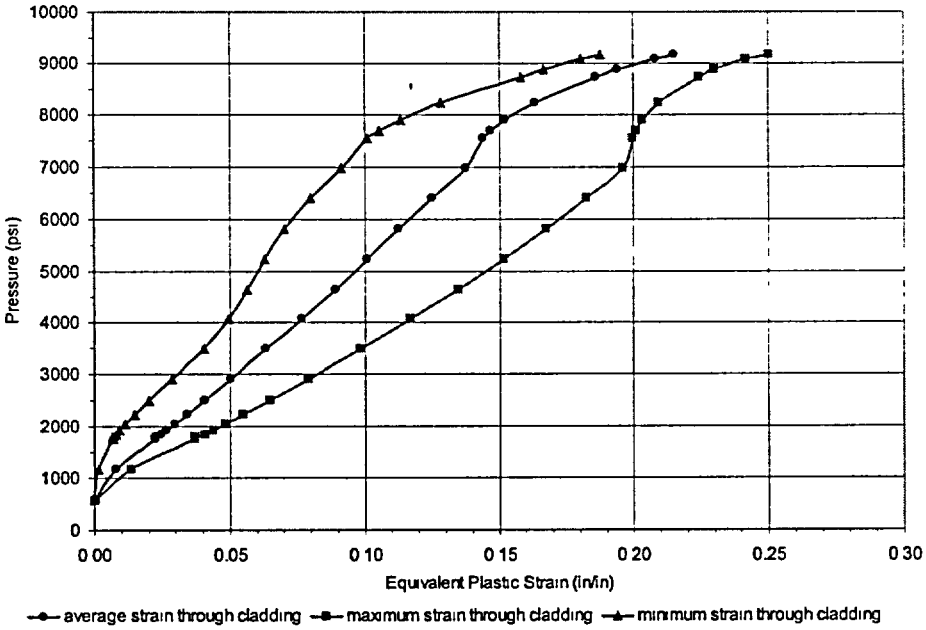

Figure A-8 Equivalent plastic strain versus pressure at the edge for corrosion diameter of 4 inches and cladding thickness of 0.188 inch

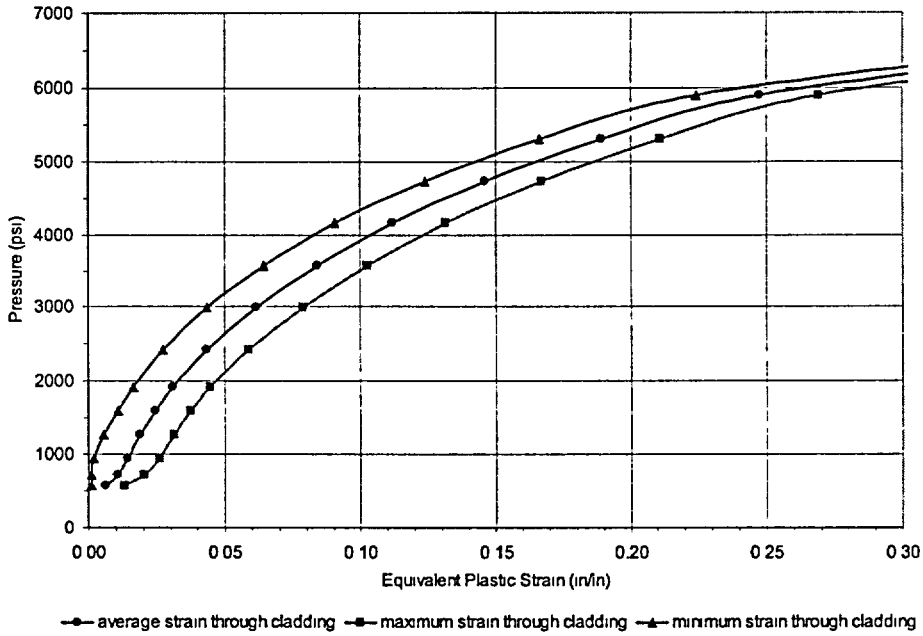

Figure A-9 Equivalent plastic strain versus pressure at the center for corrosion diameter of 4 inches and cladding thickness of 0.125 inch

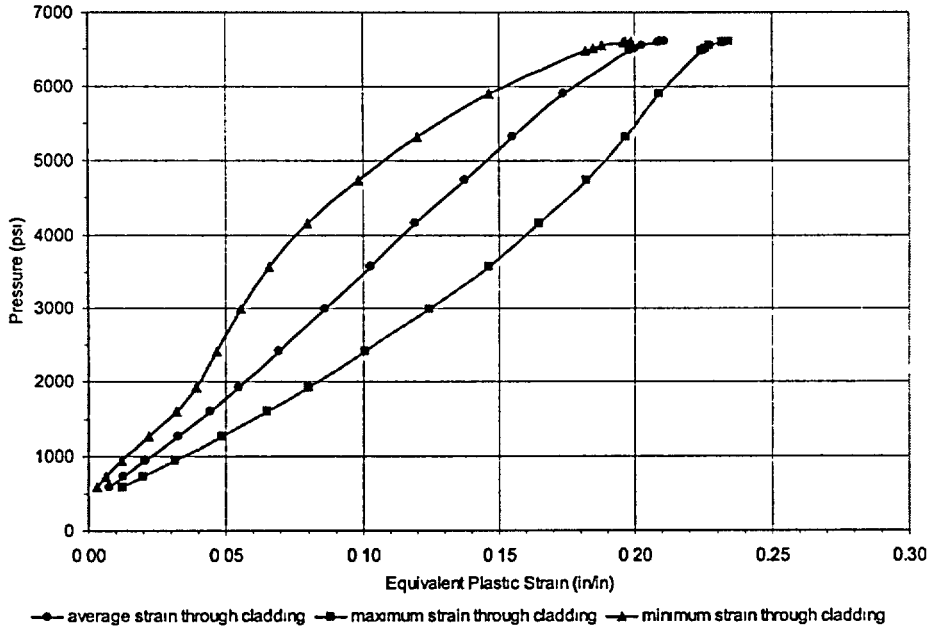

Figure A-10 Equivalent plastic strain versus pressure at the edge for corrosion diameter of 4 inches and cladding thickness of 0.125 inch

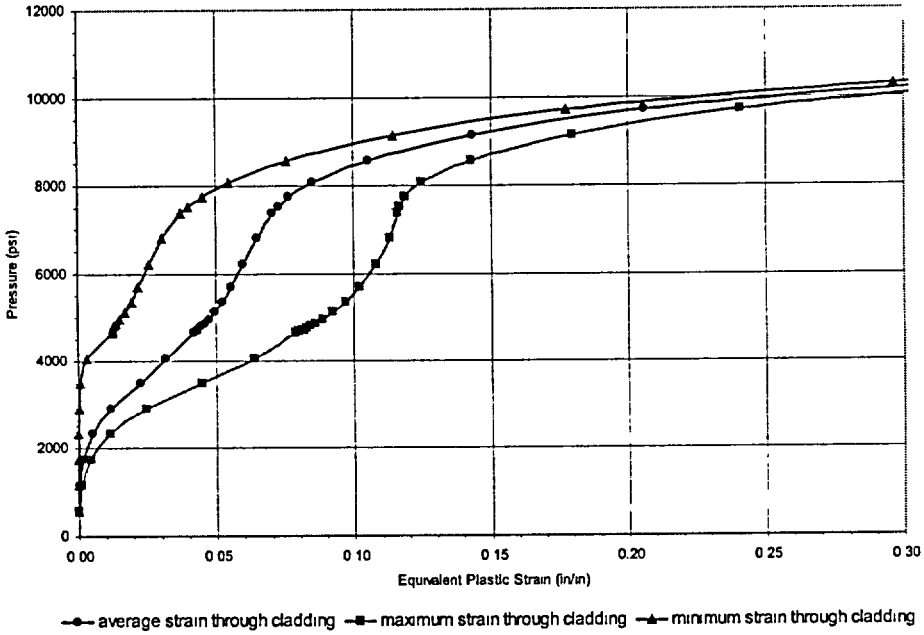

Figure A-11 Equivalent plastic strain versus pressure at the center for corrosion diameter of 5 inches and cladding thickness of 0.375 inch

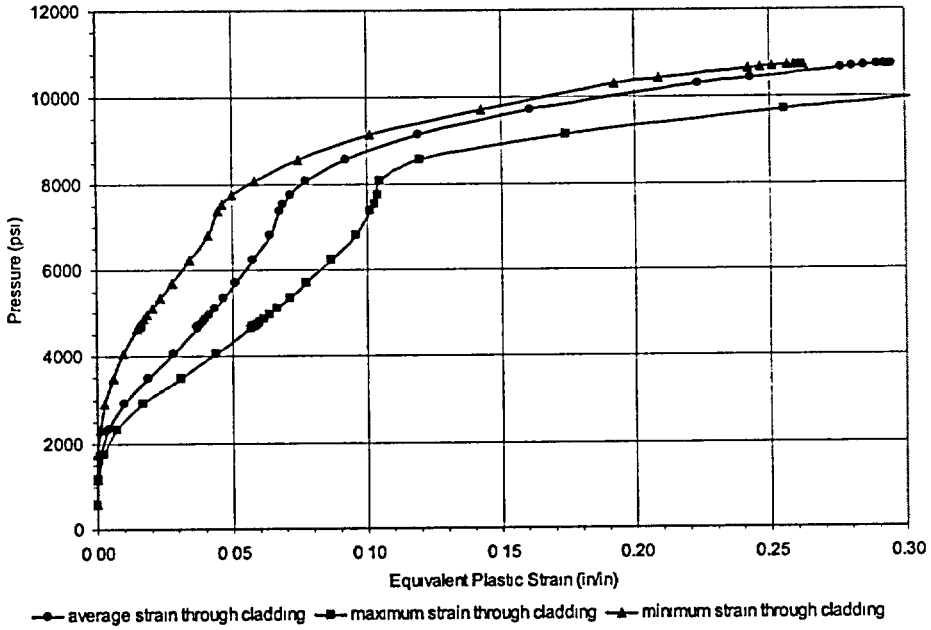

Figure A-12 Equivalent plastic strain versus pressure at the edge for corrosion diameter of 5 inches and cladding thickness of 0.375 inch

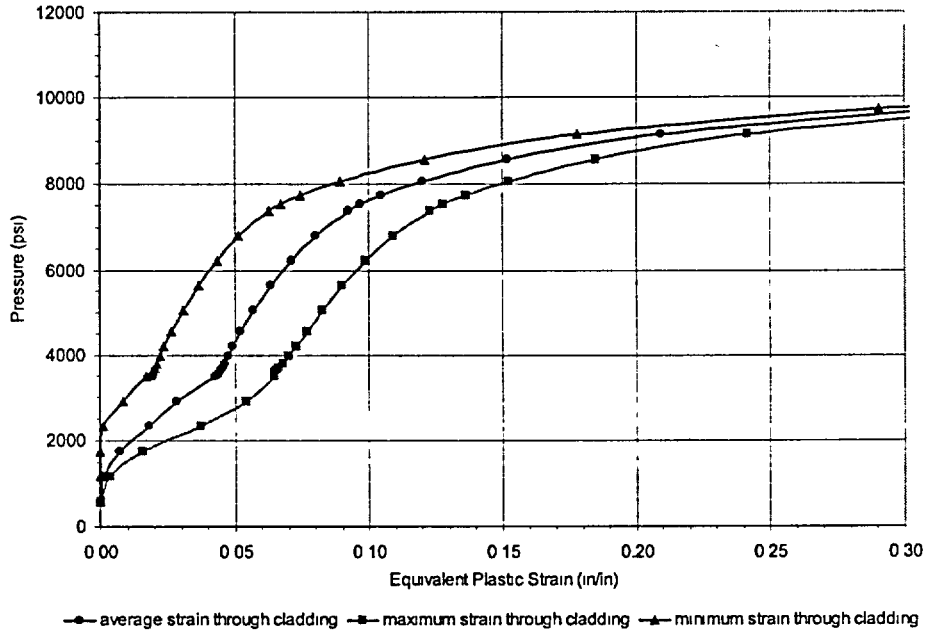

Figure A-13 Equivalent plastic strain versus pressure at the center for corrosion diameter of 5 inches and cladding thickness of 0.297 inch

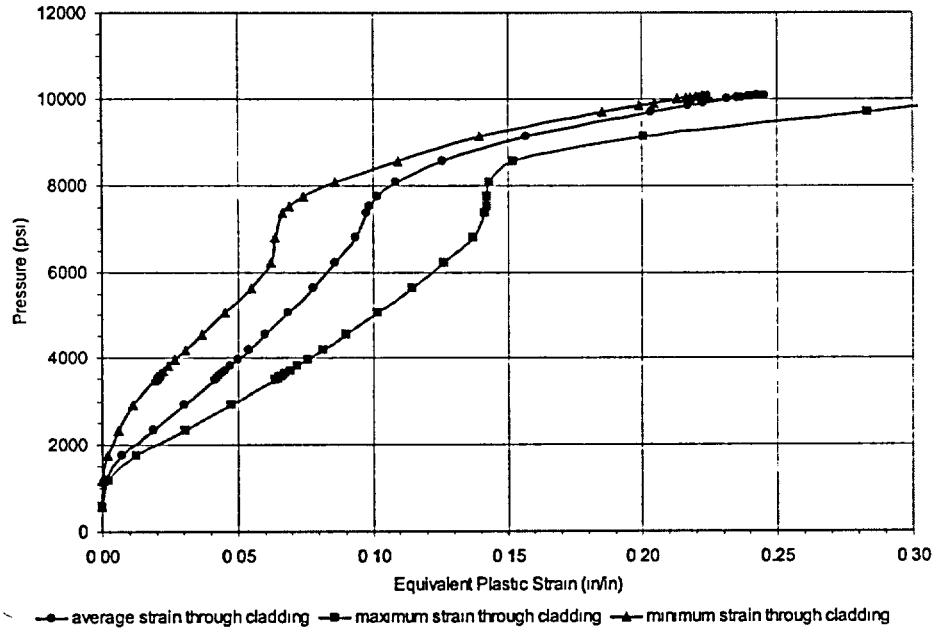

Figure A-14 Equivalent plastic strain versus pressure at the edge for corrosion diameter of 5 inches and cladding thickness of 0.297 inch

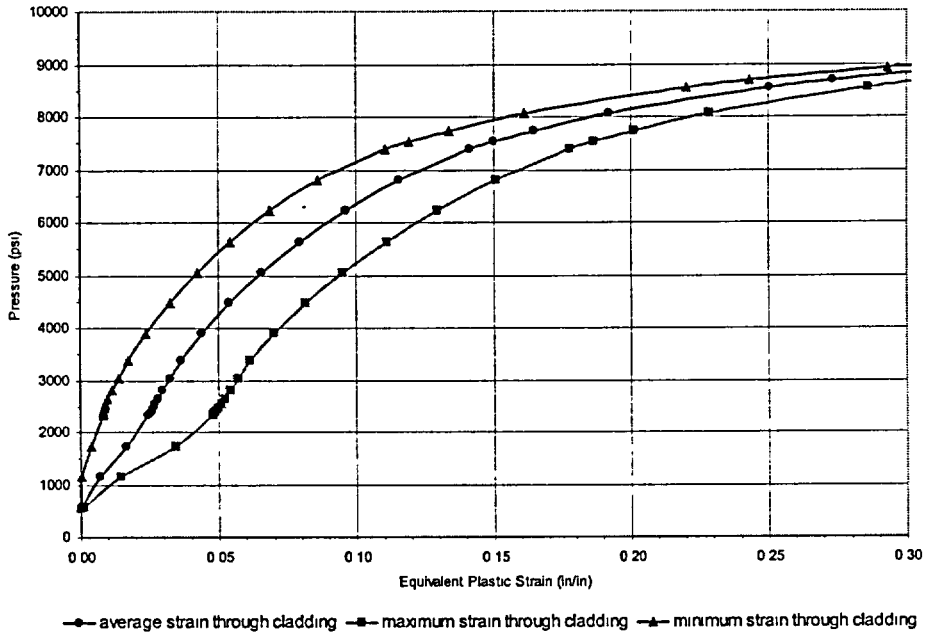

Figure A-15 Equivalent plastic strain versus pressure at the center for corrosion diameter of 5 inches and cladding thickness of 0.240 inch

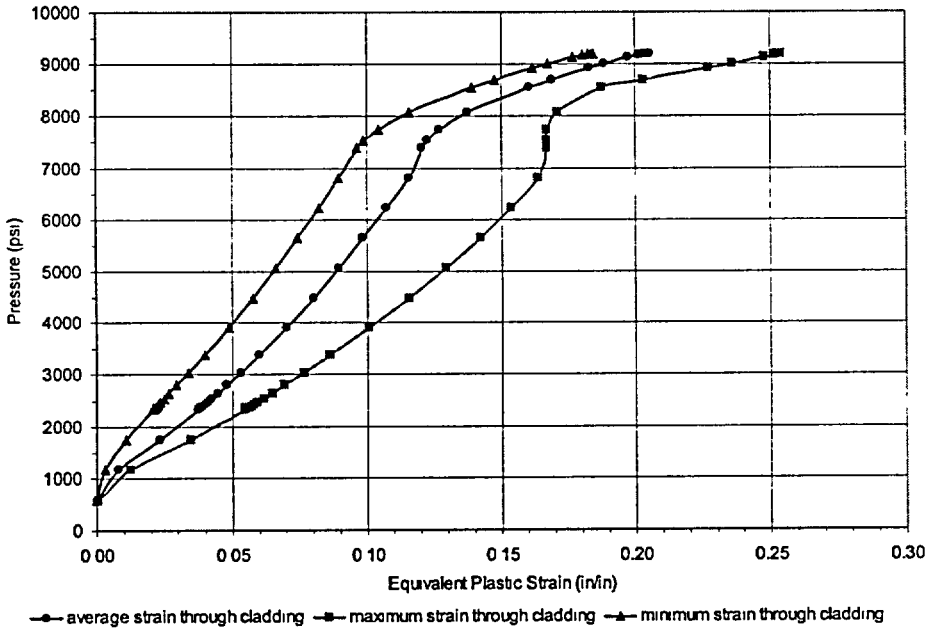

Figure A-16 Equivalent plastic strain versus pressure at the edge for corrosion diameter of 5 inches and cladding thickness of 0.240 inch

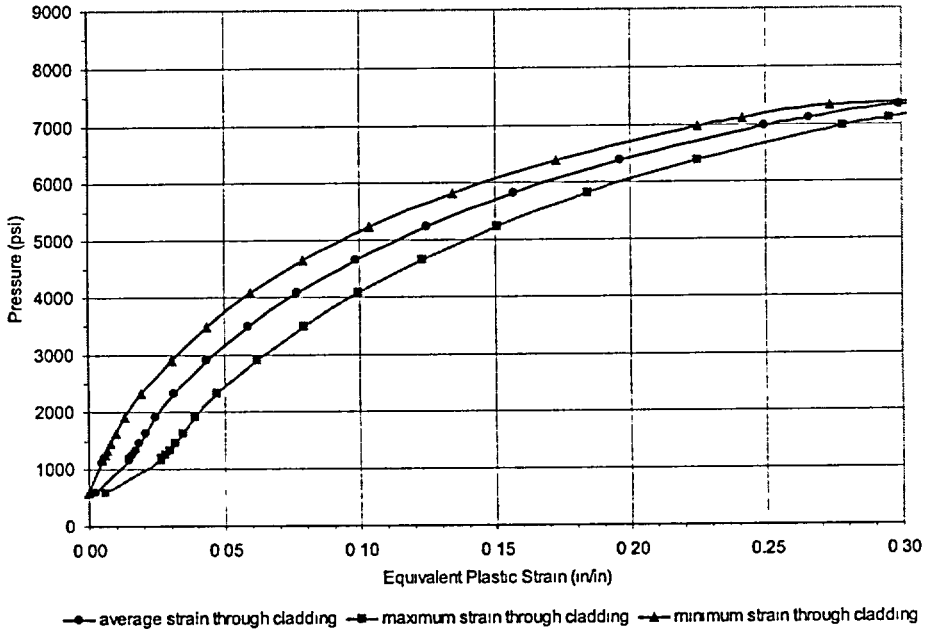

Figure A-17 Equivalent plastic strain versus pressure at the center for corrosion diameter of 5 inches and cladding thickness of 0.188 inch

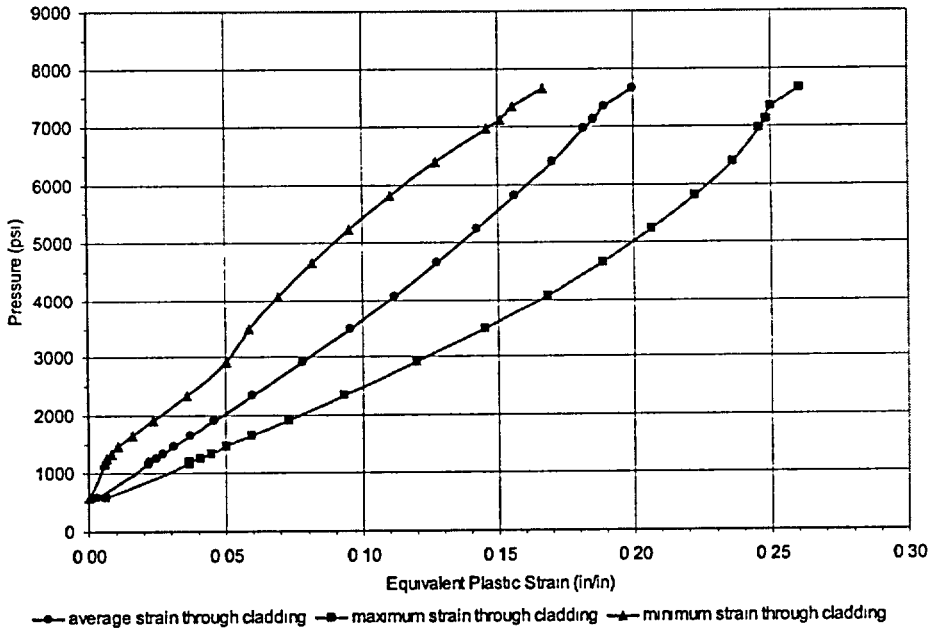

Figure A-18 Equivalent plastic strain versus pressure at the edge for corrosion diameter of 5 inches and cladding thickness of 0.188 inch

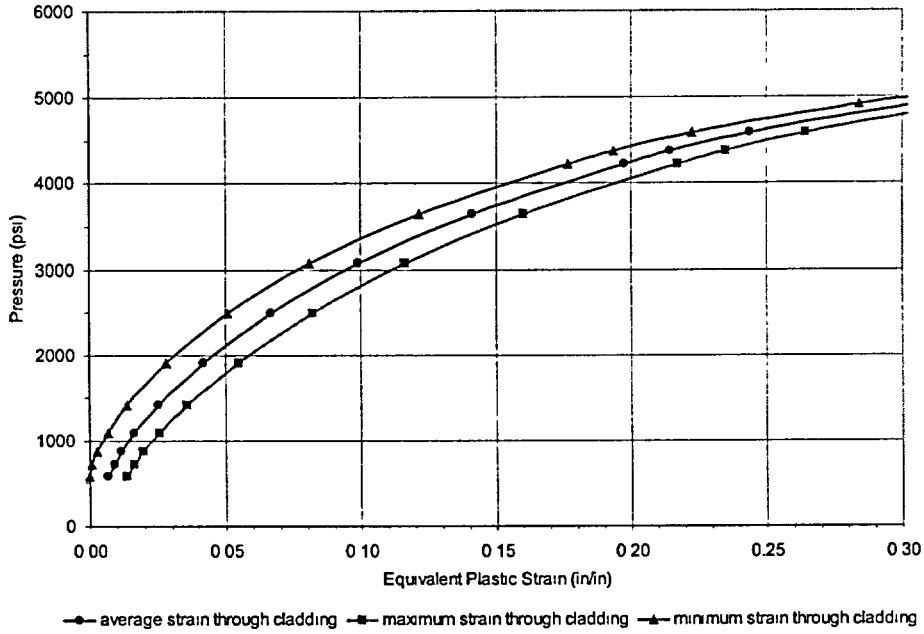

Figure A-19 Equivalent plastic strain versus pressure at the center for corrosion diameter of 5 inches and cladding thickness of 0.125 inch

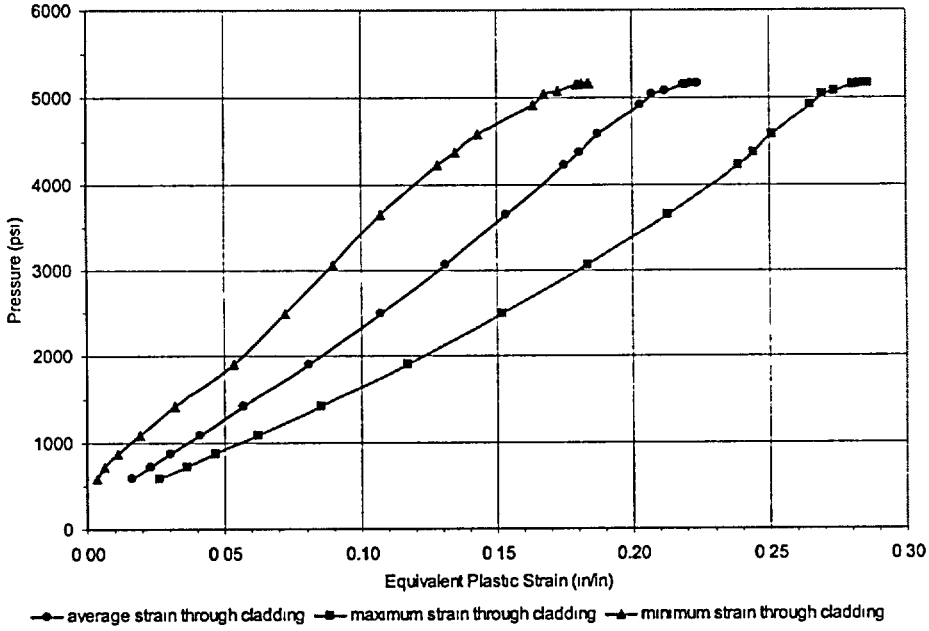

Figure A-20 Equivalent plastic strain versus pressure at the edge for corrosion diameter of 5 inches and cladding thickness of 0.125 inch

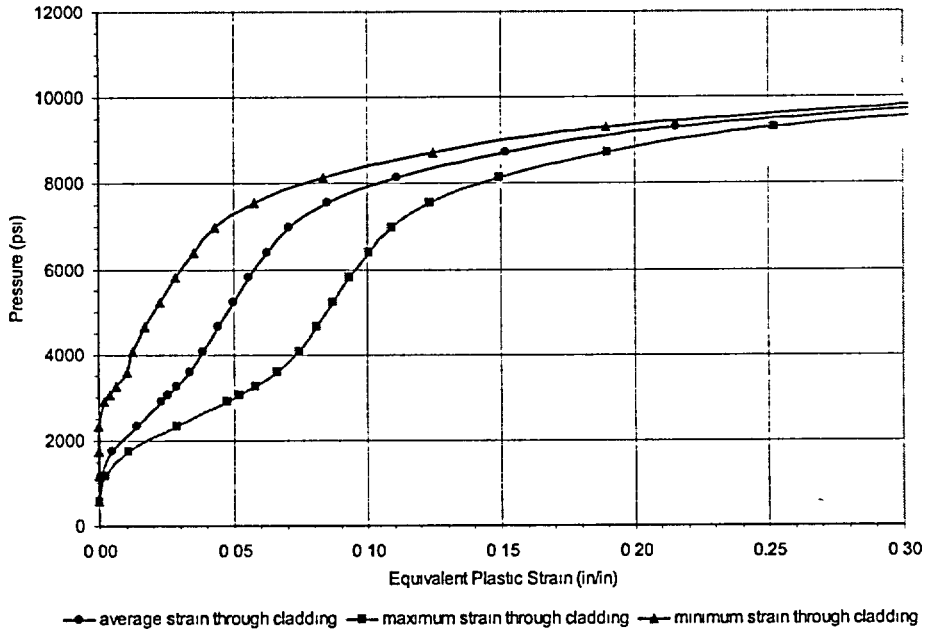

Figure A-21 Equivalent plastic strain versus pressure at the center for corrosion diameter of 6 inches and cladding thickness of 0.375 inch

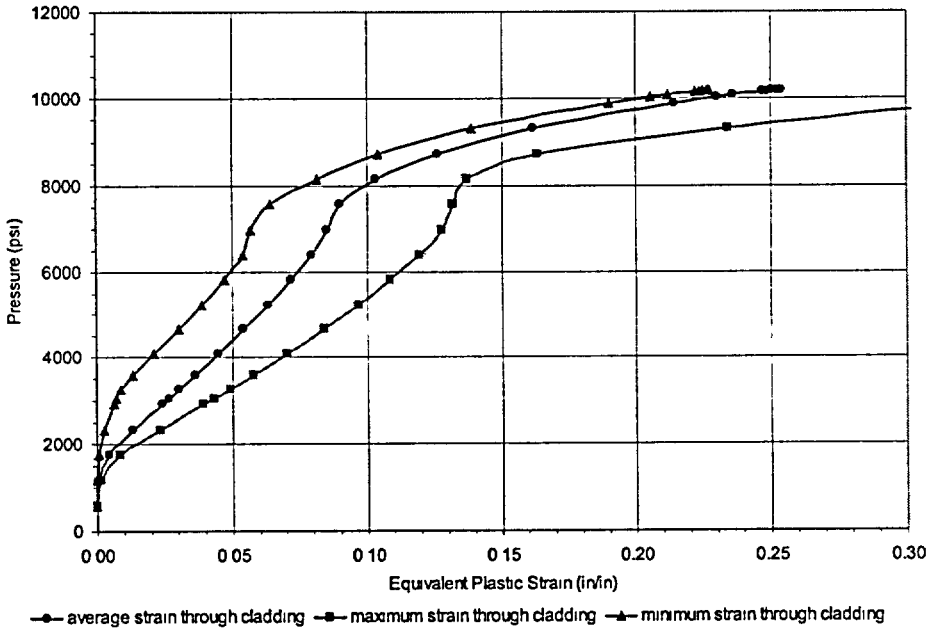

Figure A-22 Equivalent plastic strain versus pressure at the edge for corrosion diameter of 6 inches and cladding thickness of 0.375 inch

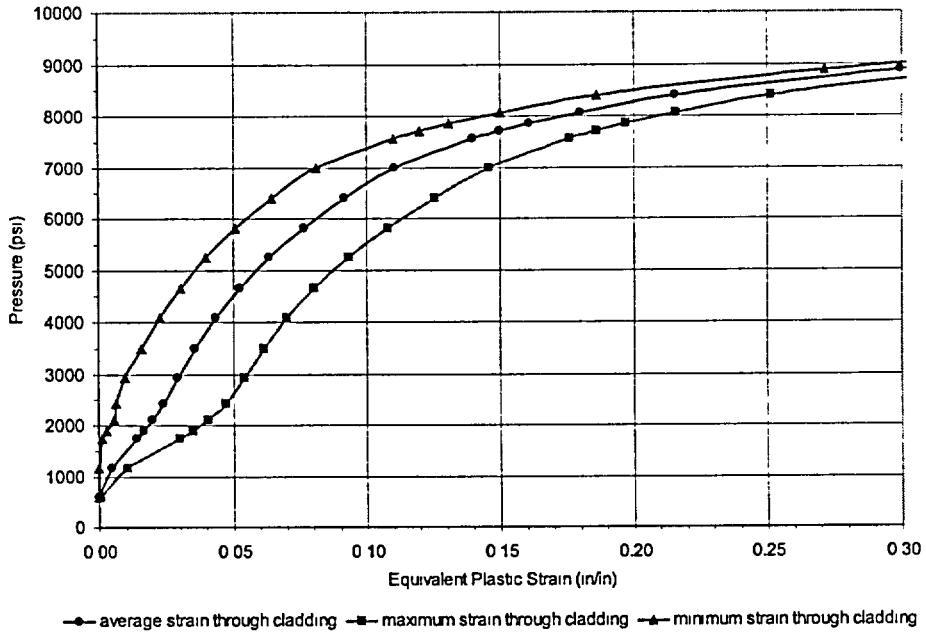

Figure A-23 Equivalent plastic strain versus pressure at the center for corrosion diameter of 6 inches and cladding thickness of 0.297 inch

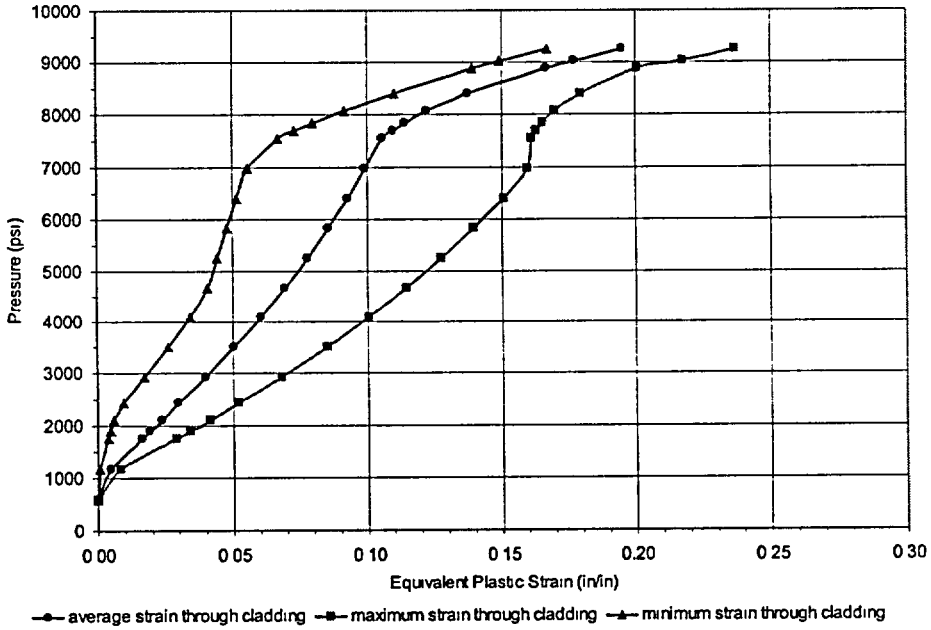

Figure A-24 Equivalent plastic strain versus pressure at the edge for corrosion diameter of 6 inches and cladding thickness of 0.297 inch

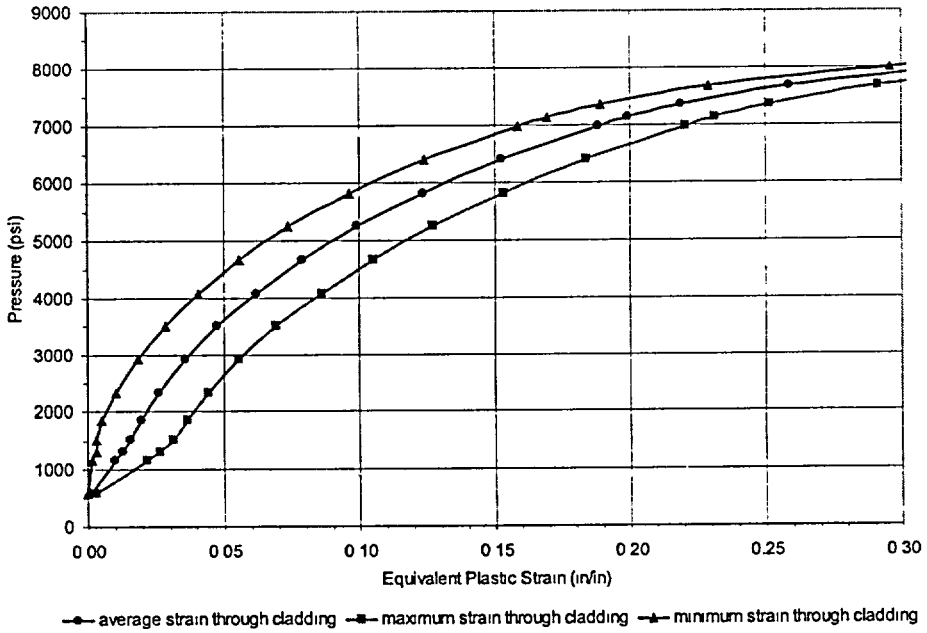

Figure A-25 Equivalent plastic strain versus pressure at the center for corrosion diameter of 6 inches and cladding thickness of 0.240 inch

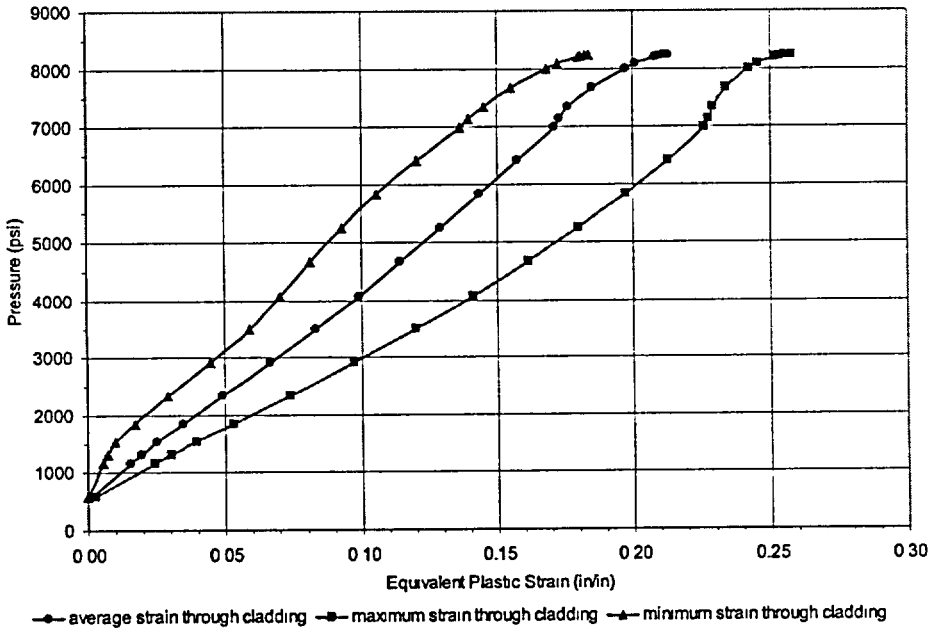

Figure A-26 Equivalent plastic strain versus pressure at the edge for corrosion diameter of 6 inches and cladding thickness of 0.240 inch

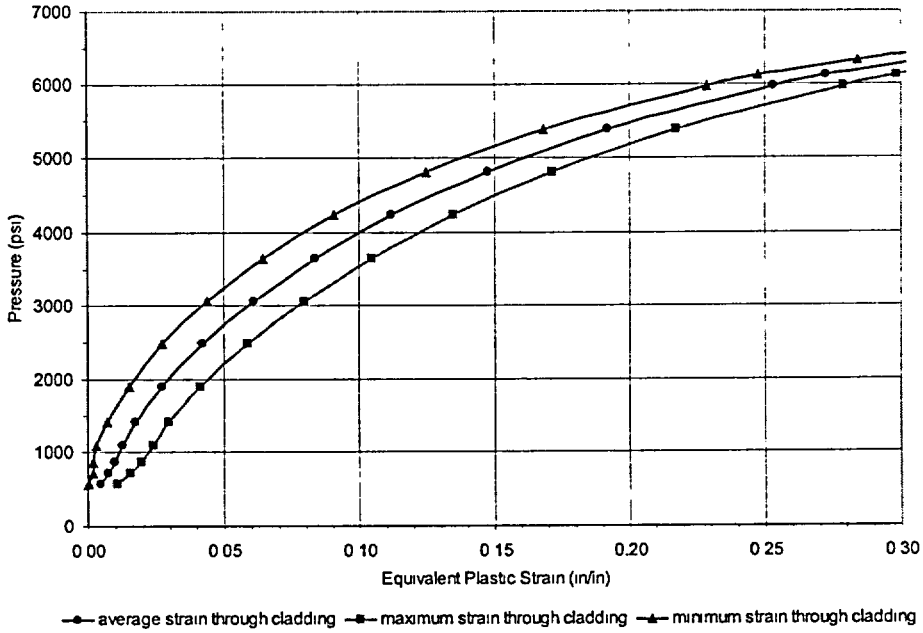

Figure A-27 Equivalent plastic strain versus pressure at the center for corrosion diameter of 6 inches and cladding thickness of 0.188 inch

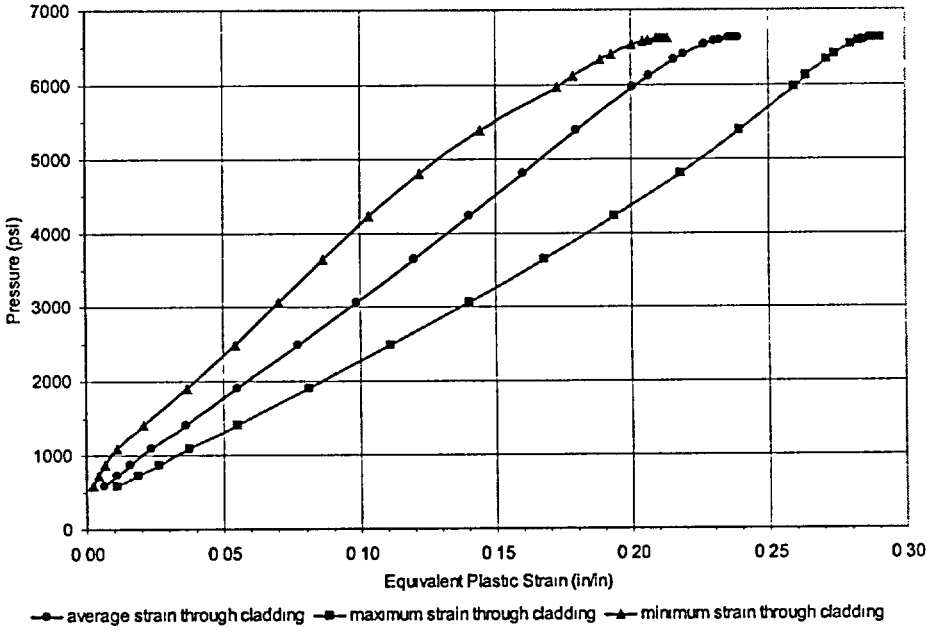

Figure A-28 Equivalent plastic strain versus pressure at the edge for corrosion diameter of 6 inches and cladding thickness of 0.188 inch

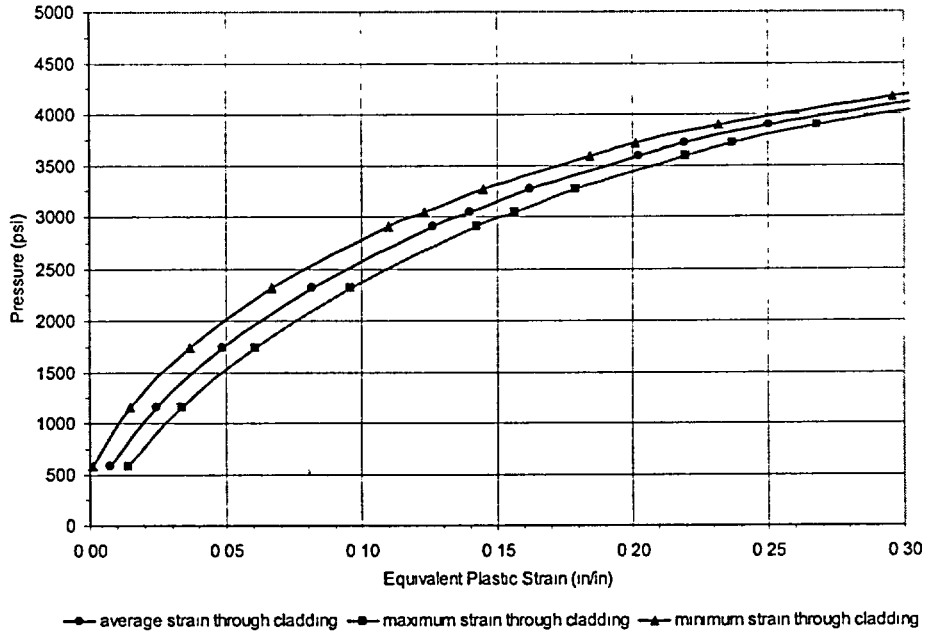

Figure A-29 Equivalent plastic strain versus pressure at the center for corrosion diameter of 6 inches and cladding thickness of 0.125 inch

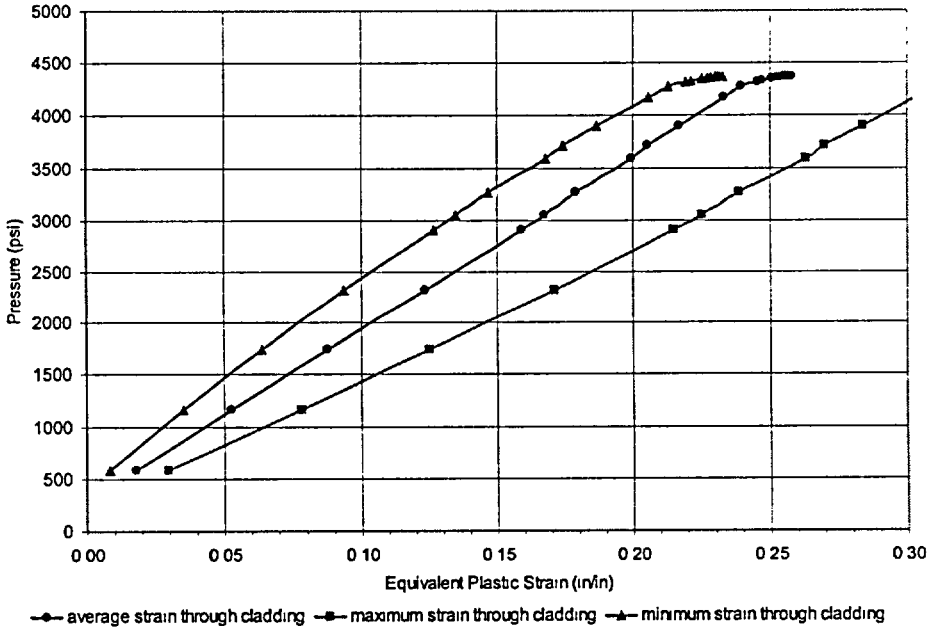

Figure A-30 Equivalent plastic strain versus pressure at the edge for corrosion diameter of 6 inches and cladding thickness of 0.125 inch

APPENDIX B

Plots of Equivalent Plastic Strain versus Pressure at the Center of the Cladding Area for the Small Deformation Analyses

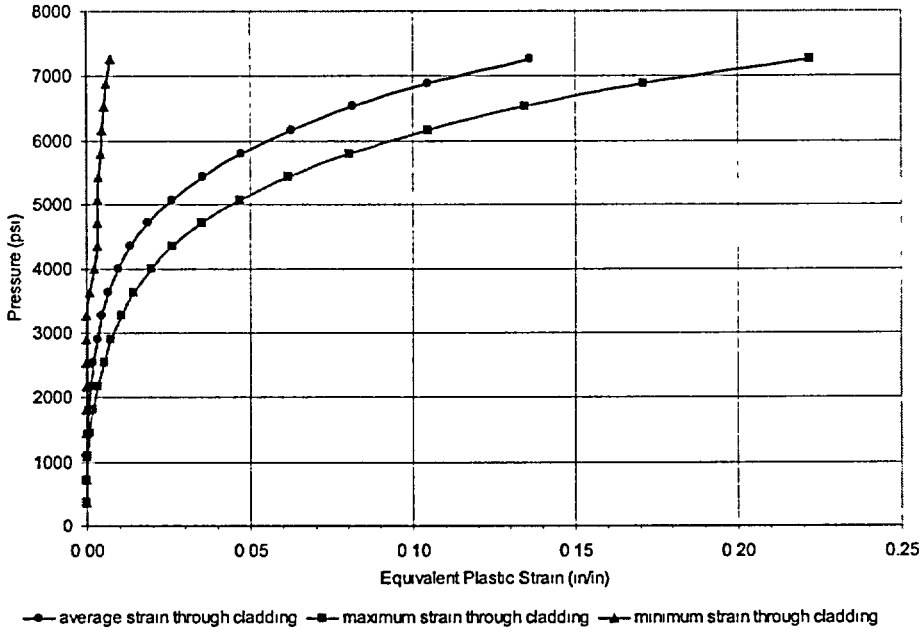

Figure B 1 Equivalent plastic strain versus pressure for corrosion diameter of 4 inches and cladding thickness of 0.375 inch

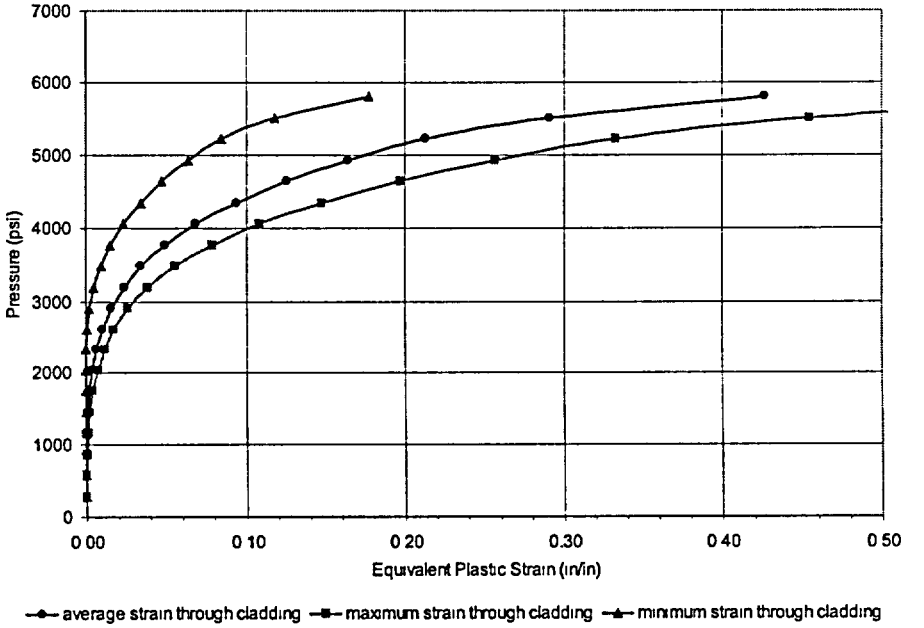

Figure B 2 Equivalent plastic strain versus pressure for corrosion diameter of 4 inches and cladding thickness of 0.297 inch

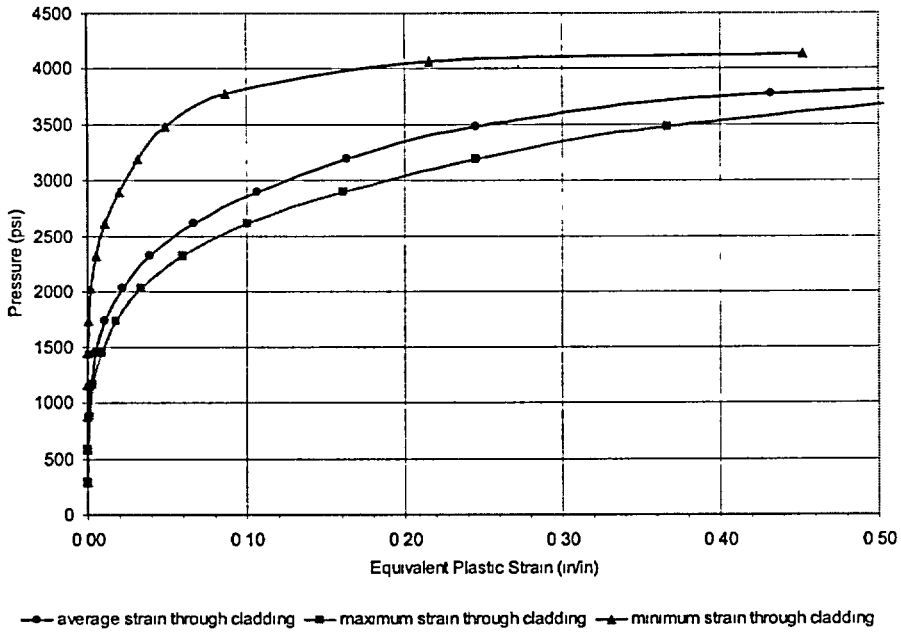

Figure B 3 Equivalent plastic strain versus pressure for corrosion diameter of 4 inches and cladding thickness of 0.240 inch

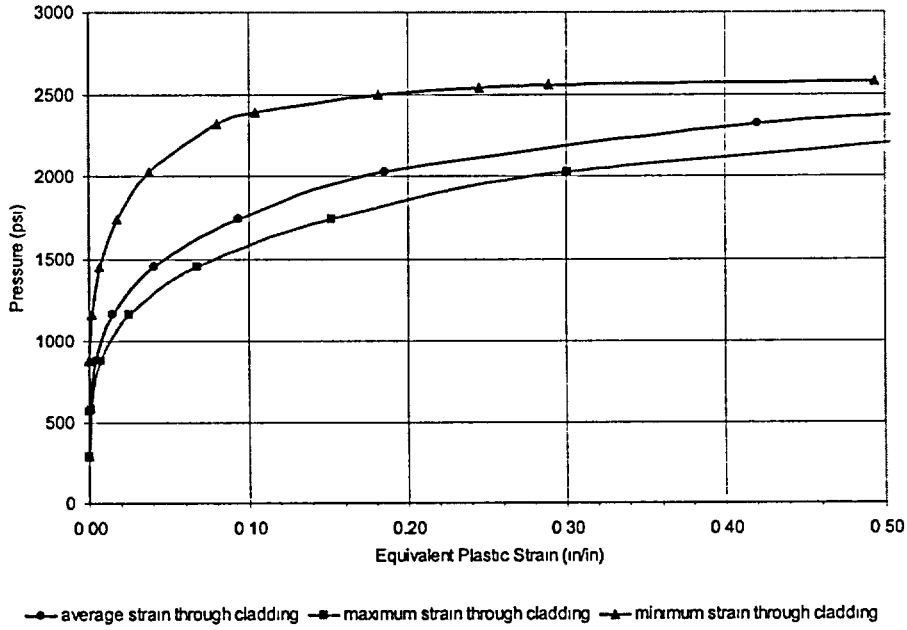

Figure B 4 Equivalent plastic strain versus pressure for corrosion diameter of 4 inches and cladding thickness of 0.188 inch

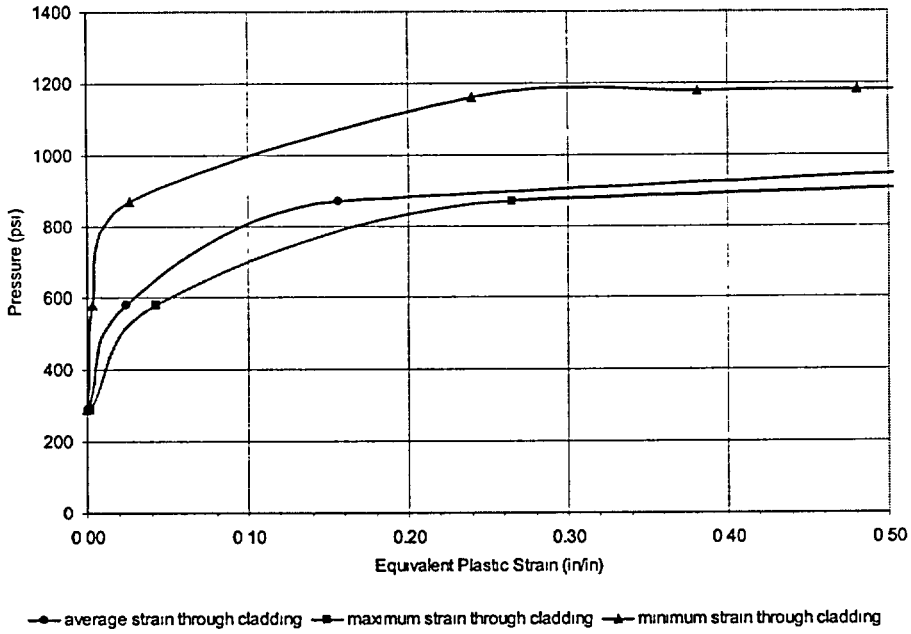

Figure B 5 Equivalent plastic strain versus pressure for corrosion diameter of 4 inches and cladding thickness of 0.125 inch

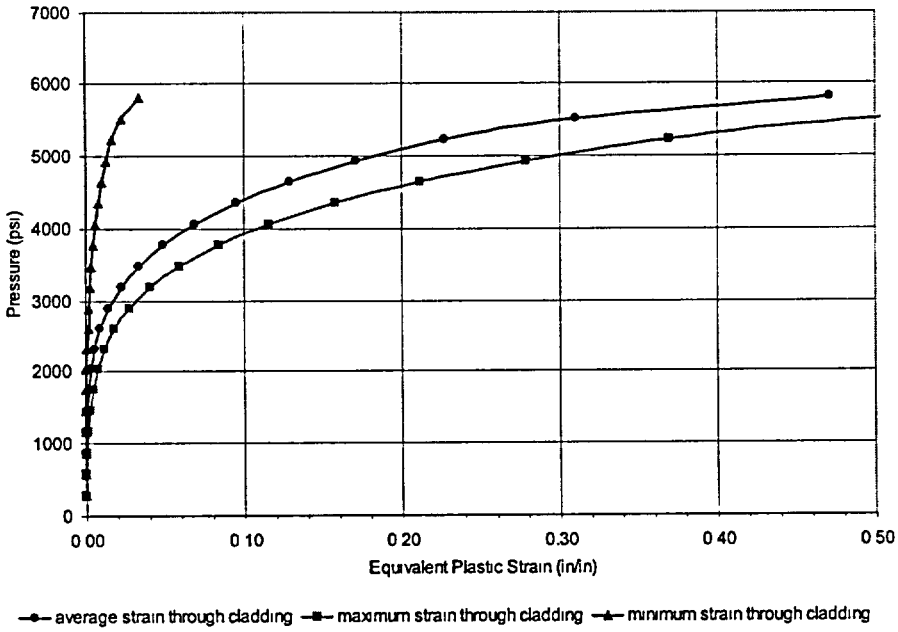

Figure B 6 Equivalent plastic strain versus pressure for corrosion diameter of 5 inches and cladding thickness of 0.375 inch

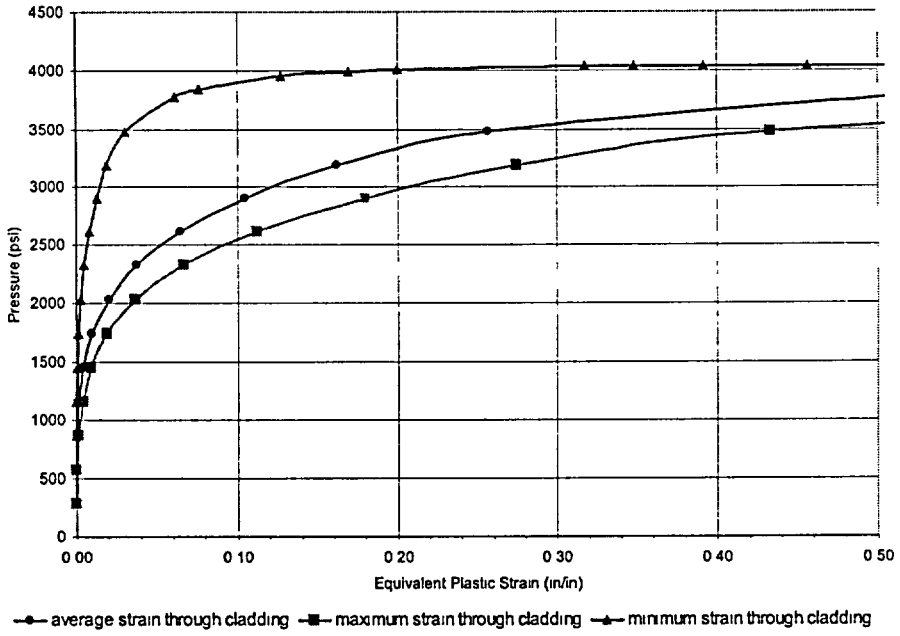

Figure B 7 Equivalent plastic strain versus pressure for corrosion diameter of 5 inches and cladding thickness of 0.297 inch

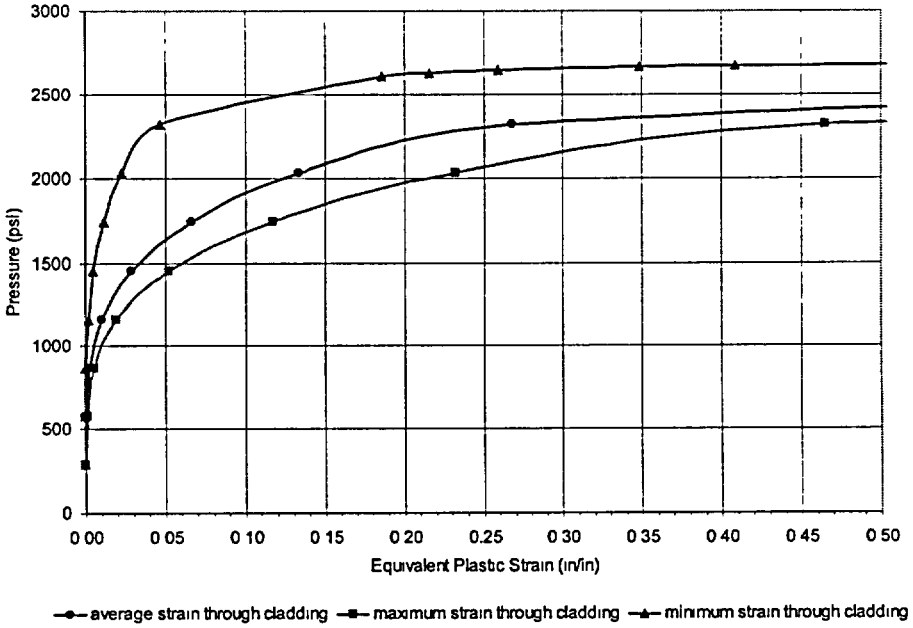

Figure B 8 Equivalent plastic strain versus pressure for corrosion diameter of 5 inches and cladding thickness of 0.240 inch

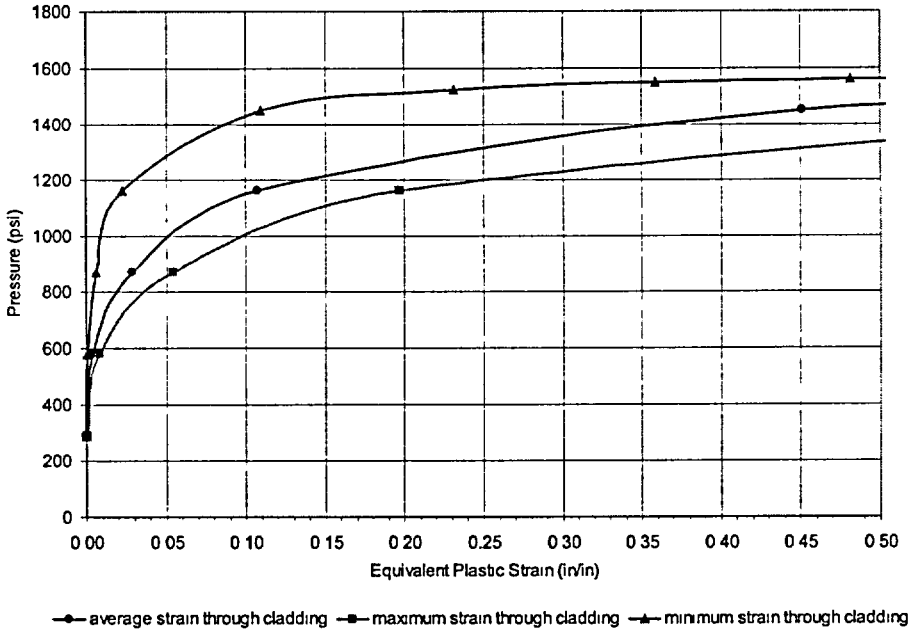

Figure B 9 Equivalent plastic strain versus pressure for corrosion diameter of 5 inches and cladding thickness of 0.188 inch

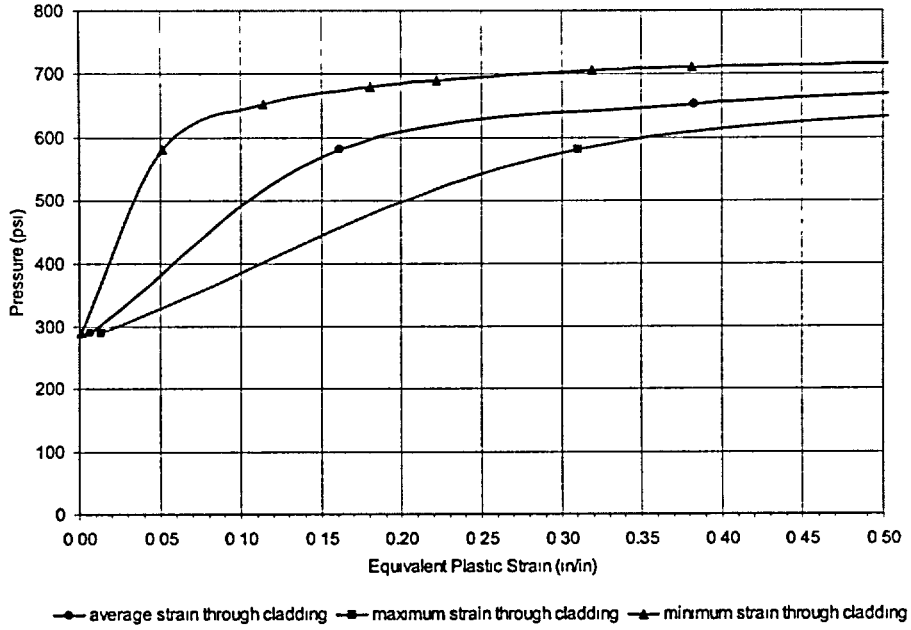

Figure B 10 Equivalent plastic strain versus pressure for corrosion diameter of 5 inches and cladding thickness of 0.125 inch

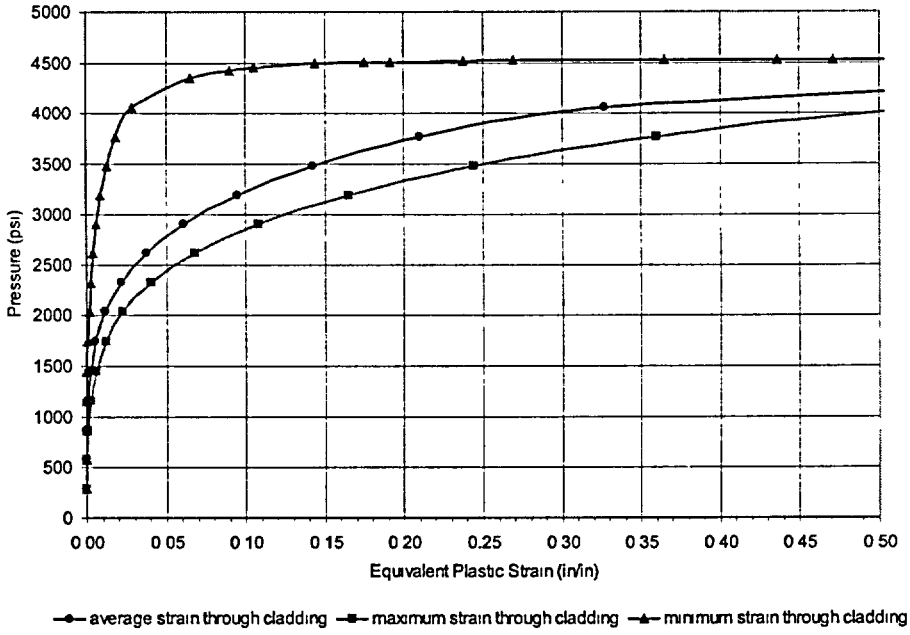

Figure B 11 Equivalent plastic strain versus pressure for corrosion diameter of 6 inches and cladding thickness of 0.375 inch

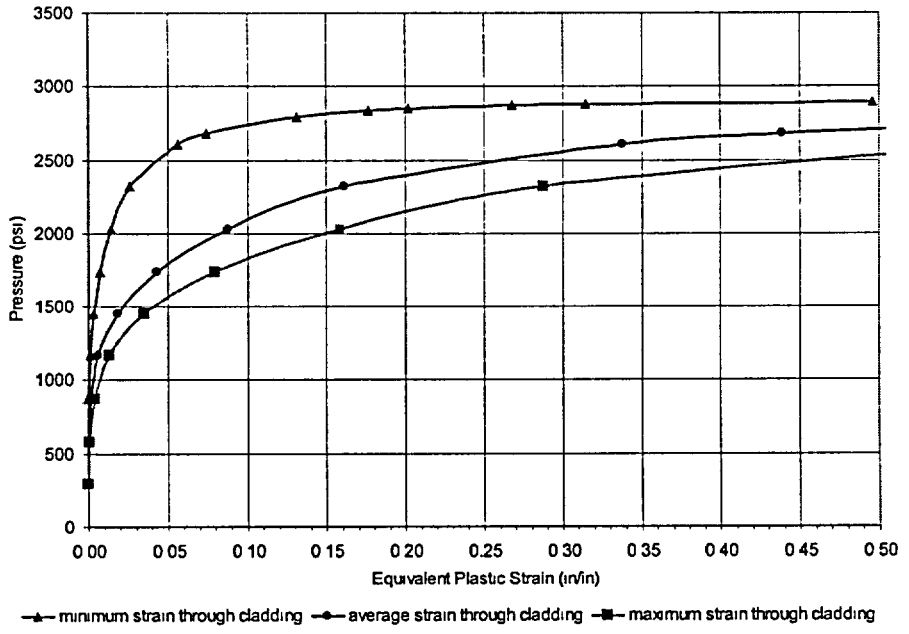

Figure B 12 Equivalent plastic strain versus pressure for corrosion diameter of 6 inches and cladding thickness of 0.297 inch

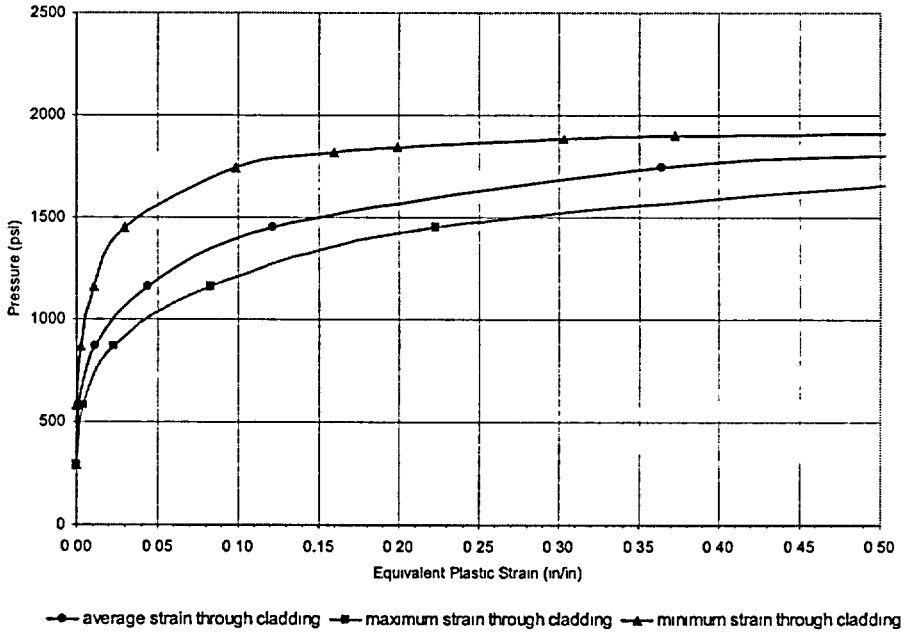

Figure B 13 Equivalent plastic strain versus pressure for corrosion diameter of 6 inches and cladding thickness of 0.240 inch

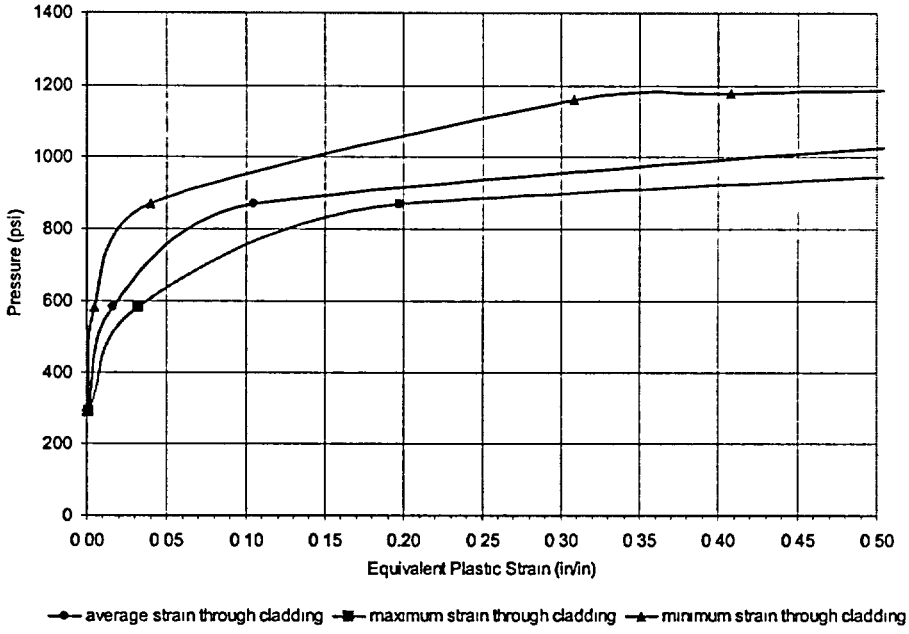

Figure B 14 Equivalent plastic strain versus pressure for corrosion diameter of 6 inches and cladding thickness of 0.188 inch

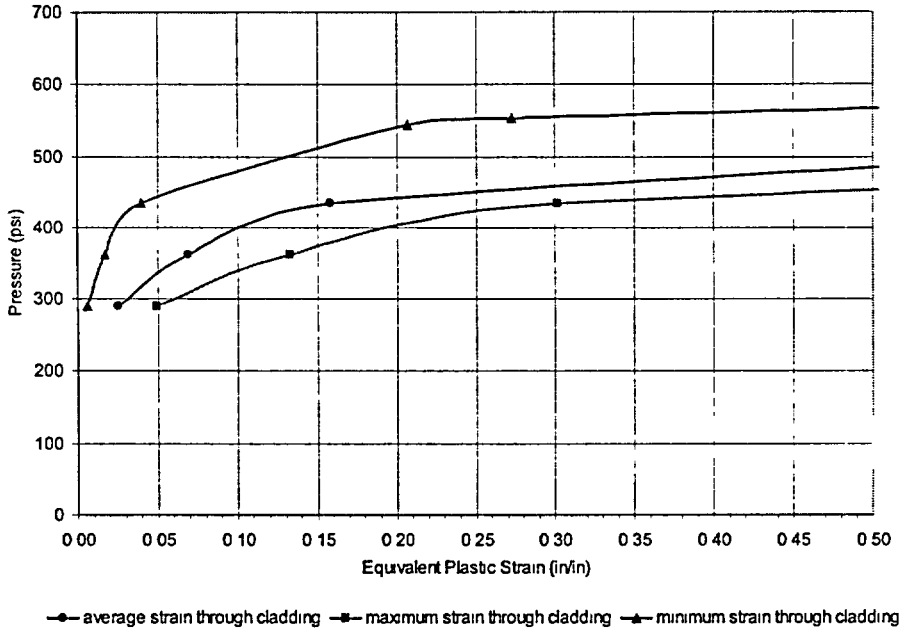

Figure B 15 Equivalent plastic strain versus pressure for corrosion diameter of 6 inches and cladding thickness of 0.125 inch

Emc²

Engineering Mechanics Corporation of Columbus
3518 Riverside Drive
Suite 202
Columbus, Ohio 43221

Phone: (614) 459-3200x228 *Fax: (614) 459-6800* *E-mail: gwilkows@columbus.rr.com*

April 30, 2002

Mr. Wallace Norris
Project Officer
U.S. Nuclear Regulatory Commission
Research, Mail Stop T-10E10
Washington, DC 20555

Dear Mr. Norris:

This report documents our short-term analysis efforts to assess the margins that might have existed for the case of the RPV head corrosion on the Davis-Besse plant.

Please contact me if you have any questions or comments.

Best Regards,

Gery M. Wilkowski

Dr. Gery M. Wilkowski
President
Engineering Mechanics Corporation of Columbus